Quantities, Units, and Ionising Radiation Fundamentals

Summary

The general concepts of quantities and units are introduced.

The advantages of the International System of Units (SI) are mentioned, and reference made to the realisation of units for selected quantities at Standards Laboratories.

Quantities and units for the measurement of ionising radiation are then discussed in detail, with particular reference to those developed for general use.

Relationships between fluence, kerma, dose and stopping power are given, with introductions to the physics of ionising radiation interactions, and including the Bragg-Gray and Spencer-Attix cavity theories.

Contents

1. Fundamentals
2. Standards and calibration
3. Radioactivity
4. Radiation field
5. Radiation interactions
6. Stopping powers
7. Dosimetry
8. Cavity theory

1: Fundamentals: Quantities and units

It is important to distinguish a *quantity* from a *unit*. In everyday language the word *quantity* is understood to be some 'amount', but in the field of measurement a 'quantity' is a characterisation of a physical phenomenon in terms that are suitable for numerical expression.

A *physical quantity* is a phenomenon capable of expression as the product of a *number* and a *unit*.

A *unit* is a selected reference sample of a *quantity*.

There are seven base units: the kilogram (kg), metre (m), second (s), ampere (A), kelvin (K), mole (mol) and candela (cd).

Derived units are obtained from combinations of the base units. Derived units may have special names. However some of the special names are restricted to certain quantities, e.g. Hz (s^{-1}) is the unit of frequency, but becquerel (s^{-1}) is the unit of activity.

The Conférence Générale des Poids et Mesures (CGPM) set up by the Metre Convention is responsible for the International System of Units (SI). The International Commission on Radiation Units and Measurements (ICRU)

recommends radiation units to CGPM. The International Commission on Radiological Protection (ICRP) recommends protection level quantities.

This table shows the relationship between SI base and derived units.

Quantity	**Unit**	**Type of unit**	**Symbol**
Length	metre	SI base unit	m
Area	metre square	SI derived unit	m^2
Energy	joule	SI derived unit with special name	J (= kg m^2 s^{-2})
Absorbed dose	gray	SI derived unit with special name (restricted use)	Gy (= m^2 s^{-2})
Absorbed dose	rad	Non-SI unit	rad (= 0.01 Gy)

Within SI, all derived units can be obtained from the base units without extra numerical factors.

SI unit prefixes

Factor	Prefix	Symbol	Factor	Prefix	Symbol
10^{24}	yotta	Y	10^{-1}	deci	d
10^{21}	zetta	Z	10^{-2}	centi	c
10^{18}	exa	E	10^{-3}	milli	m
10^{15}	peta	P	10^{-6}	micro	μ
10^{12}	tera	T	10^{-9}	nano	n
10^{9}	giga	G	10^{-12}	pico	p
10^{6}	mega	M	10^{-15}	femto	f
10^{3}	kilo	k	10^{-18}	atto	a
10^{2}	hecto	h	10^{-21}	zepto	z
10^{1}	deka	da	10^{-24}	yocto	y

2: Standards and calibration

A primary standard makes an absolute measurement, whereas secondary and other reference standard instruments must be calibrated so that the calibration is traceable to the primary standard.

A primary standard measures (or realises) the quantity of interest from first principles. Primary standards for derived units, like air kerma and absorbed dose, involve some calibration, but only to make the measurement traceable to standards for base SI units (so Gy is related to J and kg, etc.). For example, a primary standard calorimeter may work by measuring the temperature rise in a known mass of graphite: It would be important to know the mass of graphite present using calibrated measuring equipment, and the temperature measuring equipment would have to be calibrated against a standard temperature scale.

The National Measurement System is the organisation of these reference standards and the calibration process into a coherent infrastructure, designed to ensure that measurements across the country as a whole are compatible. Calibration of a dosemeter involves comparing its response with that of another, more trustworthy, instrument. This process may involve some internal adjustment in order to make the dosemeter "read correctly". More often, we obtain the numerical coefficient (the ratio of what you want, divided by what you get) by which readings should be multiplied in order to give the "correct result".

In this hierarchy of standards the primary standard sits at the apex, and everything depends on its accuracy. Compatibility of measurements in different countries depends on the consistency of their respective national standards, which is tested by comparing primary standards either directly or via the BIPM in Paris, which coordinates the International Measurement System. This is formalised in a treaty called the Mutual Recognition Arrangement.

It is surprising (but reassuring!) that, despite four different methods being in use for establishing primary standards of absorbed dose to water they agree very well (within 1%). This results in a robust calibration network since it is unlikely that there are common systematic errors in the four different methods. This is in contrast to the situation with air kerma standards for high-energy photon beams, which has in the past suffered from systematic errors common to all primary standards worldwide.

3: Radioactivity

Activity A

$$A = \frac{dN}{dt} = -\lambda N \qquad 3.1$$

Where dN is the number of nuclear transformations or decay (expectation value of the number of transitions between energy states) in the time interval, dt; and λ is the decay constant.

Mathematically dN is understood to be the differential of an expectation value of the number of active nuclei N. The arguments of differential quotients are always non-stochastic quantities.

Unit: s-1

Special name for the unit of activity is the becquerel (Bq). The curie (Ci) is still often used; 1 Ci = 37 GBq.

Of course, integrating Eq. 3.1 with respect to time, one obtains the familiar

$$N(t) = N_0 e^{-\lambda(t-t_0)} \qquad 3.2$$

or equivalently,

$$A(t) = A_0 e^{-\lambda(t-t_0)} \qquad 3.3$$

where $A(t)$ is the activity at some time t, and A_0 is the initial activity at some time t_0.

The primary standard of activity is the 4π beta-gamma-coincidence counter at NPL. (For more information consult the references.)

Related quantities

Half-life $t_{1/2}$

$$t_{1/2} = \frac{\ln 2}{\lambda} \qquad 3.4$$

The half-life is the mean time taken for a radionuclide to decay to one half of its initial activity.

Unit: s

Mean life τ

$$\tau = \frac{1}{\lambda} \qquad 3.5$$

The mean life is the mean time for a radionuclide to decay to 1/e of its original activity.

Almost all radioactive materials used in radiotherapy are artificially made either in reactors or in accelerators. For most materials such as ^{60}Co or ^{192}Ir the dose delivered to the patient is effectively constant through the treatment (the half-life of 60Co is about 5.3 years while that of ^{192}Ir is 74 days), while for others the dose delivered is limited by the half-life of the radioactive species used. For example, ^{131}I, used in the treatment of thyroid cancers, has a half-life of 8 days, but this is delivered by being chemically targeted to the thyroid tissue and so is outside the scope of this course. This course addresses issues concerning external beam radiotherapy or brachytherapy, where either long-lived radioactive sources or accelerators are used to deliver a known dose to the patient.

In terms of the physics of what happens for radioactive decay: First, the radioactive cobalt is made in a reactor,

$$^{59}_{28}\mathrm{Co} + \mathrm{n} \rightarrow {}^{60}_{28}\mathrm{Co}$$

Then in the radiation source, the radioactive disintegration takes place. In β-decays, this takes place initially via the weak interaction, with a half-life of 5.271 years:

$$^{60}_{28}\mathrm{Co} \rightarrow {}^{60}_{28}\mathrm{Ni}^{*} + \mathrm{e}^{-} + \nu$$

The excited nickel nucleus then decays via the electromagnetic interaction, which is much stronger than the weak interaction so the decay is much more rapid, with a half-life of about 3.3 picosecond:

$$^{60}_{28}\mathrm{Ni}^{*} \rightarrow {}^{60}_{28}\mathrm{Ni} + 2\gamma$$

The two photons escape with energies of 1.17 and 1.33 MeV. It is these photons which interest us.

Other sources of photons or fast electrons may be accelerators, where electrons are accelerated to very high energy and then either used to irradiate a patient directly in electron beam radiotherapy, or to generate high-energy bremsstrahlung photons which are then heavily filtered before irradiating the patient.

4: Radiation field

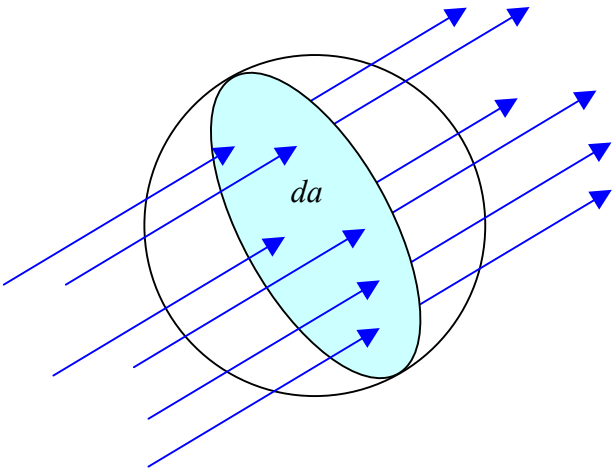

Fig 1 Illustration of particle fluence

Fluence Φ

A number of particles passing a surface, constitutes a fluence. It is defined as

$$\Phi = \frac{dN}{da} \qquad 4.1$$

where dN is the number of particles incident on a sphere of cross-sectional area da. The use of a sphere expresses the fact one considers the area perpendicular to the direction of each particle. The fluence is independent of the incident angle of the radiation.

Unit: m^{-2}

Planar fluence is the number of particles crossing a plane per unit area and hence does depend on the angle of incidence of the particles.

Energy fluence Ψ

$$\Psi = \frac{dE}{da} \qquad 4.2$$

where dE is the radiant energy incident on a sphere of cross-sectional area da.

Unit: $J\ m^{-2}$

Note: Energy is often expressed in units of electron volts, symbol eV. 1 eV is equal to the energy gained by an electron in passing through a potential difference of 1 volt. This is not an SI unit, but is accepted for use with the SI. 1 eV is approximately 1.602×10^{-19} joule.

For a monoenergetic beam, $\Psi = \Phi E$, where E is the energy of the beam.

Fluence differential in energy $\Phi_E(E)$

For a beam with a spectrum of energies it is useful to extend the concepts to fluence differential in energy, or the distribution of fluence with respect to energy, $\Phi_E(E)$.

$$\Phi_E(E) = \frac{d\Phi}{dE}(E) \qquad 4.3$$

where $d\Phi$ is the fluence of particles with energy between E and $E + dE$.

Unit: $m^{-2}\ J^{-1}$

Similarly the energy fluence differential in energy $\Psi_E(E)$ can be defined

$$\Psi_E(E) = \frac{d\Psi}{dE}(E) = \frac{d\Phi}{dE}(E)E \qquad 4.4$$

Figure 2 illustrates the relationship between particle fluence Φ_E and energy fluence Ψ_E, both as functions of energy, for a particular spectrum of X-rays.

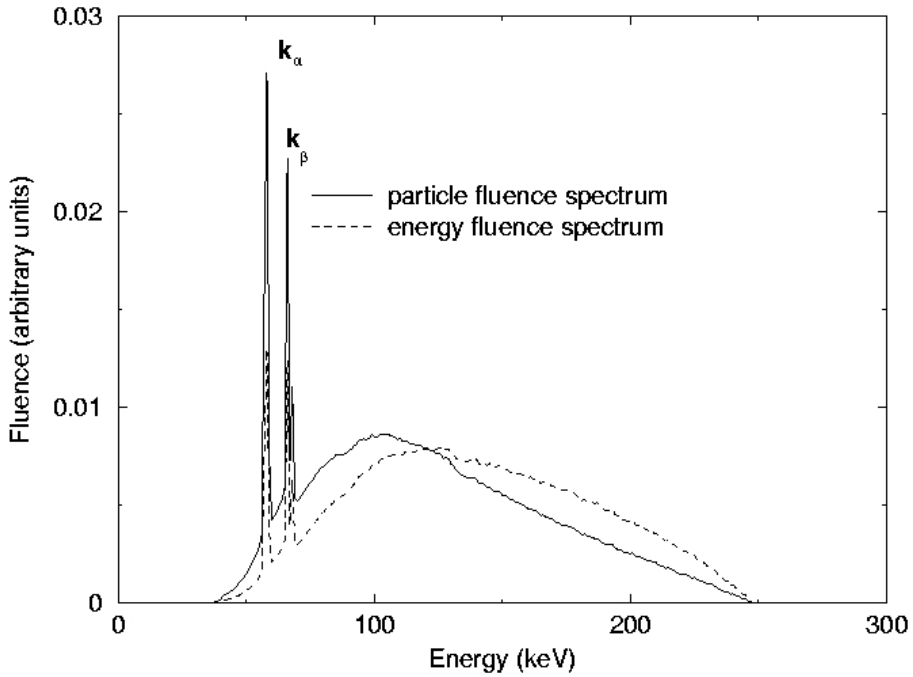

Fig. 2 Photon fluence and energy fluence spectra at 1 m from the target of an x-ray machine with tube potential 250 kV and added filtration of 1 mm Al and 1.8 mm Cu (target material: W; inherent filtration 2 mm Be).

A complete description of a radiation field requires the fluence distribution as a function of: (i) particle type e.g. electrons, photons, neutrons (this may include any relevant quantum state, e.g. spin), (ii) spatial position, (iii) direction, (iv) energy and (v) time.

The rate quantities e.g. fluence rate, tend to have their own symbols. Up to now we have described only scalar quantities; it is possible to define and use vector quantities, e.g. vectorial fluence $\bar{\Phi}$.

5: Dosimetry

The energy of photons is imparted to matter in a two-stage process. In the first stage the photon energy transfers to electrons; in the second stage the electrons transfer energy to the medium through ionisations and atomic excitations.

Kerma *K* (from the acronym ***K***inetic ***E***nergy ***R***eleased per unit ***Ma***ss) quantifies the first stage, where the energy is transferred from indirectly ionising radiation to directly ionising radiation.

For most radiotherapy applications this happens through Compton scattering interactions, where the photon scatters off atomic electrons leading to a photon of reduced energy scattered away at some angle and an energetic electron slowing down in the medium.

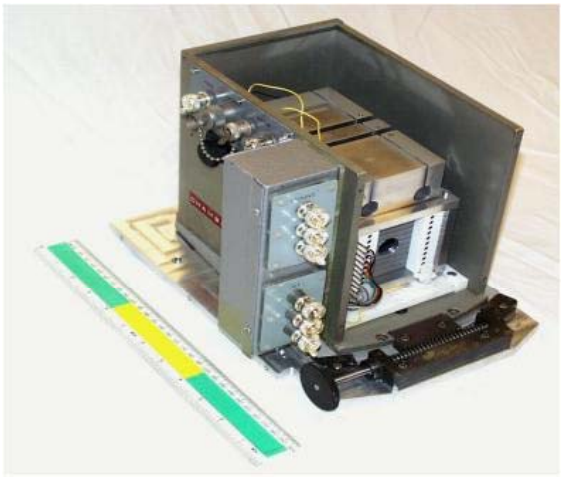

Fig 3 Primary standard of air kerma for 50 kV X-rays

At higher energies (as may be delivered from high-energy bremsstrahlung X-ray treatments from accelerators), a significant fraction of the interactions will be through pair production, where the photon passes close enough to the cell nucleus that it interacts with the nuclear electric field, leading to the production of an electron-positron pair. These energetic particles slow down in the medium delivering the dose, and at the end of the track the positron will annihilate with an electron with the emission of two back-to-back photons with energy 511 keV.

The main photon interactions in materials may be illustrated thus:

Photoelectric effect:

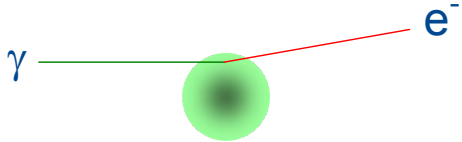

Low-energy photons

Ejects a single atomic electron

$E_e = E_\gamma$ - binding energy

This effect dominates at low energies, up to a few tens of keV.

Compton scattering:

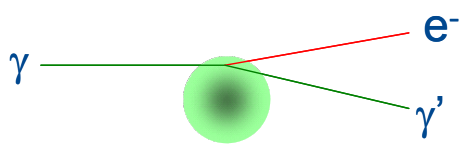

Medium-energy photons

Ejects a single atomic electron

$$E_{\gamma'} = \frac{E_\gamma}{1+\alpha(1-\cos\theta)}$$

$$E_e = E_\gamma \frac{m_0c^2(1-\cos\theta)}{1+m_0c^2(1-\cos\theta)}$$

where $\alpha = E_\gamma/m_0c^2$ (m_0c^2 is the mass-energy of the electron, 0.511 MeV) and θ is the photon scattering angle. The minimum scattered photon energy occurs at $\theta = 180°$, with the maximum scattered electron energy at 0°, and these are given by

$$E_{\gamma',\min} = E_\gamma \frac{1}{1+2\alpha} \text{ and } E_{e,\max} = E_\gamma \frac{2\alpha}{1+2\alpha}.$$

The Compton effect dominates at medium energies from a few tens of keV up to several MeV in low-Z materials such as water, graphite, or tissue.

Pair production:

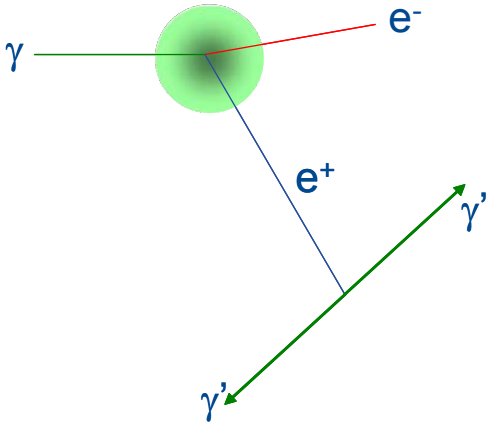

Only for high-energy photons,

E_γ > 1.022 MeV

$E_\gamma = E_{e-} + E_{e+}$ + 1.022 MeV

More prominent with high-Z material as the interaction is almost always with te nuclear electric field.

The positron slows down in the medium, and then annihilates with an atomic electron, with the resultant emission of two back-to-back 0.511 MeV photons.

Occasionally at higher energies, triplet production can occur, where the incoming photon interacts with an atomic electron rather than the nucleus. Also of course at higher energies, photoactivation an occur where the incoming photon interacts with the nuclear field to produce an excited compound nucleus, which may decay by the emission of (most commonly) a neutron, leaving an unstable nucleus which will then break up via radioactive decay later on. This is rare in low-Z materials such as water or tissue, which at least means we are less likely to make the patient radioactive.

Figure 4 shows the relative interaction probabilities in water or tissue, for photons up to 10 MeV. Above 20 MeV, pair production becomes dominant.

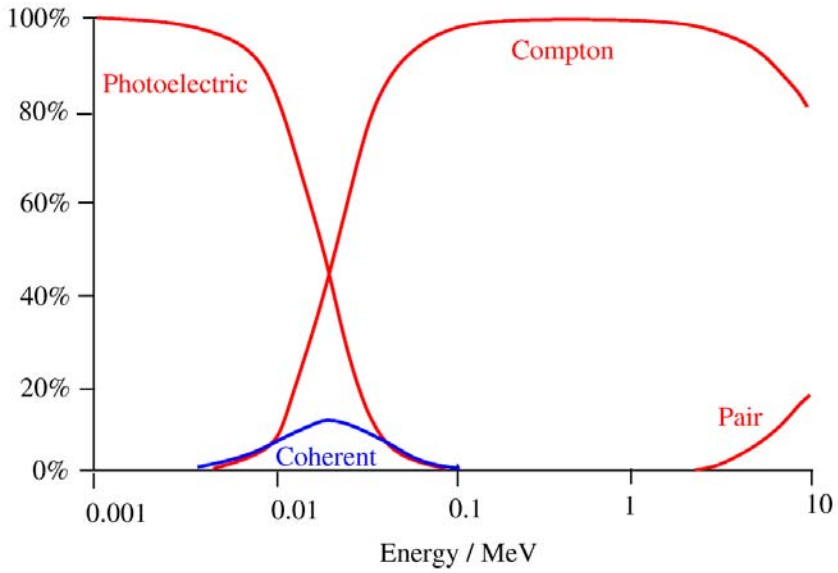

Fig 4 Relative interaction probabilities of photons in low-Z material such as water or tissue.

Kerma is defined as:

$$K = \frac{d\overline{E}_{tr}}{dm} \qquad 5.1$$

where $d\overline{E}_{tr}$ is the mean kinetic energy transferred to charged particles via the interactions described above, from uncharged particles in a mass dm. The medium should always be specified. There are various primary standards to realise K for various particle types (photons, electrons, protons and other light nuclei) and energies (a few tens of keV for X-rays, up to hundreds of MeV for protons and light nuclei).

Unit: J kg-1

The special name for the unit of kerma is gray (Gy)

Kerma relationship to fluence

For monoenergetic photons, the kerma is given by

$$K = \Psi \frac{\mu_{tr}}{\rho} \qquad 5.2$$

The kerma is usually expressed in terms of the distribution $\Psi_E(E)$ of the uncharged energy fluence with respect to energy. The kerma K is then given by

$$K = \int \Psi_E(E) \frac{\mu_{tr}(E)}{\rho} dE \qquad 5.3$$

where $\frac{\mu_{tr}(E)}{\rho}$ is the tabulated calculated mass energy transfer coefficient of the material for uncharged particles of energy E. From this, the ratio of kerma in two materials where the fluence ratio is the same (through proper scaling of

dimensions) is equal simply to the ratio of average mass energy transfer coefficients (the scaling theorem).

Total kerma can be split into two parts: *collisional kerma* and *radiative kerma*. Collisional kerma K_{coll} leads to the production of electrons that dissipate their energy as ionisation near electron tracks in the medium, and it is this component that delivers the absorbed dose within a medium. Radiative kerma K_{rad} leads to the production of bremsstrahlung as the charged particles are decelerated in the medium.

The collisional kerma K_{coll} is given by

$$K_{coll} = \int \Psi_E(E) \frac{\mu_{en}(E)}{\rho} dE \qquad 5.4$$

where $\frac{\mu_{en}(E)}{\rho}$ is the tabulated calculated mass energy absorption coefficient of the material for uncharged particles of energy E.

This may be rewritten in a form similar to eq. 5.2:

$$K_{coll} = \Psi \frac{\overline{\mu}_{en}}{\rho} \qquad 5.5$$

where

$$\Psi = \int_0^{E_{\max}} \Psi_E(E) dE \qquad 5.6$$

is the total (integrated) energy fluence and

$$\frac{\overline{\mu}_{en}}{\rho} = \frac{1}{\Psi} \int_0^{E_{\max}} \Psi_E(E) \frac{\mu_{en}(E)}{\rho} dE \qquad 5.7$$

is the mass energy absorption coefficient averaged over the energy fluence spectrum.

For selected energy fluence spectra, $\frac{\overline{\mu}_{en}}{\rho}$ may be tabulated.

Absorbed dose, *D*

Electrons travel through the medium and deposit energy along their tracks. Therefore the absorption of energy described by absorbed dose does not take place at the same location as the transfer of energy to charged particles described by kerma. The absorbed dose is defined as

$$D = \frac{d\overline{\varepsilon}}{dm} \qquad 5.8$$

where $d\overline{\varepsilon}$ is the mean energy imparted to matter of mass dm. Energy imparted is the energy incident minus the energy leaving the mass, minus the

energy released in nuclear transformations (to stop the dose becoming negative when, for example, the mass contains a radioactive source).

Unit: J kg-1. The absorbing medium should always be specified.

Special name for the unit of absorbed dose is gray (Gy).

There are various primary standards to realise the Gy for various particle types and energies. NPL currently maintains primary standard therapy level absorbed dose calorimeters for photon beams and electron beams, and is currently developing new primary standard therapy level absorbed dose calorimeters for photon and electron beams, for proton beams and for brachytherapy sources. For a more detailed review of calorimeters consult the references.

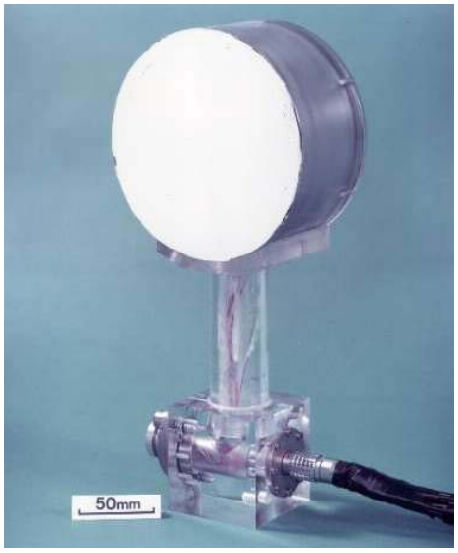

Fig 5 Primary standard of absorbed dose: The photon microcalorimeter

Kerma and dose (charged particle equilibrium)

Generally, the transfer of energy (kerma) from a photon beam to charged particles at a particular location does not lead to the absorption of energy by the medium (absorbed dose) at the same location. This is due to the finite range of the secondary electrons released through photon interactions: A 10 MeV electron for example, has a range in water of about 5 cm.

Since photons (from Compton scattering or from pair annihilation) mostly escape from the volume of interest, one relates absorbed dose usually to collisional kerma. In general, the ratio of dose and collisional kerma will be denoted as:

$$\beta = \frac{D}{K_{coll}} \qquad 5.9$$

If the photons from radiative kerma escape the volume of interest, it is assumed that $\beta \approx 1$.

Figure 6 illustrates the relation between collisional kerma and absorbed dose for a high energy photon beam under build-up conditions; (a) under conditions of charged particle equilibrium (CPE), and (b) under conditions of transient charged particle equilibrium (TCPE). As a high-energy photon beam penetrates the medium, collisional kerma is maximal at the surface of the irradiated material because photon fluence is greatest at the surface. Initially, the charged particle fluence, and hence the absorbed dose, increases as a function of depth until the depth of dose maximum (z_{max}) is attained.

This build-up of absorbed dose is responsible for the skin sparing effect in the case of high energy photon beams. However, in practice the surface dose is small but does not equal zero, because of the electron contamination in the beam due to photon interactions in the media upstream from the phantom or due to charged particles generated in the accelerator head and beam modifying devices.

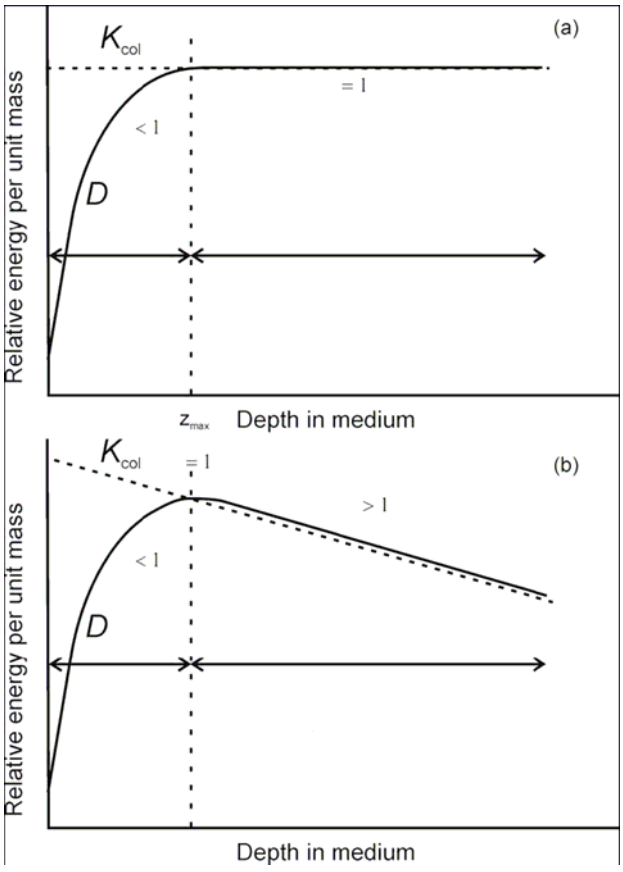

Fig. 6 Collision kerma and absorbed dose as a function of depth in a medium irradiated by a high energy photon beam: (a) With no photon attenuation (hypothetical). (b) With photon attenuation.

If there were no photon attenuation or scattering in the medium, but yet production of electrons, the hypothetical situation where the build-up region is followed by a region of complete CPE where $D = K_{coll}$ would occur.

In the more realistic situation, however, due to photon attenuation and scattering in the medium, a region of TCPE occurs, where there exists an

essentially constant relation between collisional kerma and absorbed dose. This relation is practically constant since, in high energy photon beams, the average energy of the generated electrons and hence their range, do not change appreciably with depth in the medium.

In the special case where true charged particle equilibrium does exist, at the depth of maximum dose in the medium z_{max}, the relation between absorbed dose D and total kerma K is given by:

$$D = K_{coll} = K(1-\bar{g}) \qquad 5.10$$

where $\bar{g}$ is the bremsstrahlung fraction, depending on the electron kinetic energy; the higher the energy, the larger is $\bar{g}$. The bremsstrahlung fraction also depends on the material considered, with higher values of $\bar{g}$ for higher Z materials. For electrons produced by cobalt-60 gamma rays in air the bremsstrahlung fraction is 0.0032.

6: Charged particles – Stopping powers

'Stopping power' is actually a misnomer because dimensionally, it is a force. The ICRU is considering changing the name to "retarding force".

Stopping powers are calculated for electrons and positrons using the Bethe theory for "soft" collisions, with the stopping power as a result of "hard" collisions calculated using Møller cross-sections for electrons and Bhabha cross-sections for positrons.

A "soft" collision occurs when a charged particle passes an atom at a considerable distance, i.e. $b>>a$ where b is the impact parameter and a is the atomic radius. Only a very small amount of energy is transferred to an atom of the absorbing medium in a single collision.

In a "hard" collision where $b \cong a$, a secondary electron (often referred to as a delta electron) with considerable energy is ejected and forms a separate track.

According to ICRU Report 37, the complete mass collisional stopping power for electrons and photons is

$$\frac{S_{coll}}{\rho} = \frac{N_A Z}{A}\frac{\pi r_0^2 2m_e c^2}{\beta^2}\left[\ln\left(\frac{E_K}{I}\right)^2 + \ln\left(1+\frac{\tau}{2}\right) + F^{\pm}(\tau) - \delta\right] \qquad 6.1$$

with F^- for electrons given as

$$F^-(\tau) = (1-\beta^2)\left[1+\frac{\tau^2}{8} - (2\tau+1)\ln 2\right]$$

and F^+ for positrons given as

$$F^+(\tau) = 2\ln 2 - \frac{\beta^2}{12}\left[23 + \frac{14}{\tau+2} + \frac{10}{(\tau+2)^2} + \frac{4}{(\tau+2)^3}\right]$$

where $\tau = E_K/m_e c^2$ and $\beta = v/c$.

The density effect correction δ in Eq. 6.1 accounts for the polarisation of the medium caused by the passing of a charged particle, which reduces the effective Coulomb force exerted on that particle. This affects the soft collision component of the stopping power. It is significant in the calculation of the ratio of stopping powers between media of different densities, such as that between water and air, and various models have been developed for it. The references contain more information on this.

The linear stopping power is defined as the expectation value of the rate of energy loss per unit path length dE/dx of the charged particle. The mass stopping power is defined as the linear stopping power divided by the density of the absorbing medium. Convenient units for the linear and the mass stopping powers are MeV/cm and MeV·cm^2/g, respectively.

There are two types of stopping powers: *collisional* resulting from interactions of charged particles with atomic orbital electrons; and *radiative* resulting from interactions of charged particles with atomic nuclei, giving rise to the production of bremsstrahlung. These may be illustrated thus:

Collisional stopping power:

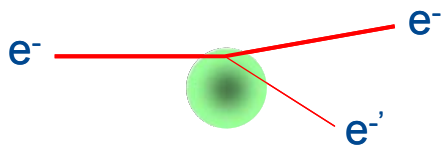

Energy loss by ionisation

Dominates for lower energies and low-Z material

Absorbed dose delivered to material via this process

Radiative stopping power:

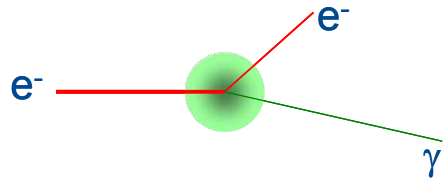

Scattering, mainly by nuclei

Energy loss by photon emission (bremsstrahlung)

Dominates for higher energies and high-Z material

Radioactivation can also occur with high-energy electrons but the probability is significantly lower than with photons; in essence, a bremsstrahlung photon has to be generated in the nuclear field which then may interact with the nucleus as described for photoactivation (page 9) to give an excited compound nucleus.

Restricted and unrestricted stopping powers

The *unrestricted mass collisional stopping power* expresses the average rate of energy loss by a charged particle in all (hard as well as soft) collisions. It is used for example in Bragg-Gray cavity theory, where the assumption is made that there is no significant contribution to the charged particle fluence from high-energy scattered electrons arising from “hard” collisions.

The concept of the *restricted mass collisional stopping power* is introduced to calculate the energy transferred to a localised region of interest. By limiting the energy transfer to secondary charged (delta) particles to a threshold Δ, highly energetic secondary particles are allowed to escape the region of interest. This is addressed in the modified cavity theory due to Spencer and Attix.

The restricted stopping power is therefore lower than the unrestricted stopping power. The choice of the energy threshold depends on the problem. For ionization chambers a frequently used threshold value is 10 keV (the range of a 10 keV electron in air is on the order of 2 mm).

The *restricted linear collisional stopping power* (also referred to as linear energy transfer) L_Δ of a material, for charged particles, is the quotient of dE_Δ by dx, where dE_Δ is the energy lost by a charged particle due to soft and hard collisions in traversing a distance dx minus the total kinetic energy of the charged particles released with kinetic energies higher than Δ:

$$L_\Delta = \frac{dE_\Delta}{dx} \qquad 6.2$$

The *restricted mass collisional stopping power* is the *restricted linear collisional stopping power* divided by the density ρ of the material.

The *total mass stopping power* is the sum of the collisional mass stopping power and the radiative mass stopping power. Figure 7 shows the total unrestricted and restricted (Δ = 10 keV and 100 keV) electron mass stopping powers for graphite based on the data in ICRU Report 37. As the threshold for maximum energy transfer in the restricted stopping power increases, the restricted mass stopping power approaches the unrestricted mass stopping power for $\Delta \rightarrow E_K/2$, where E_K represents the electron kinetic energy. Note also that, since energy transfers to secondary electrons are limited to $E_K/2$, unrestricted and restricted electron mass stopping powers are identical for kinetic energies lower than or equal to 2Δ. This is indicated in Fig. 7 with short vertical lines at 20 keV and 200 keV.

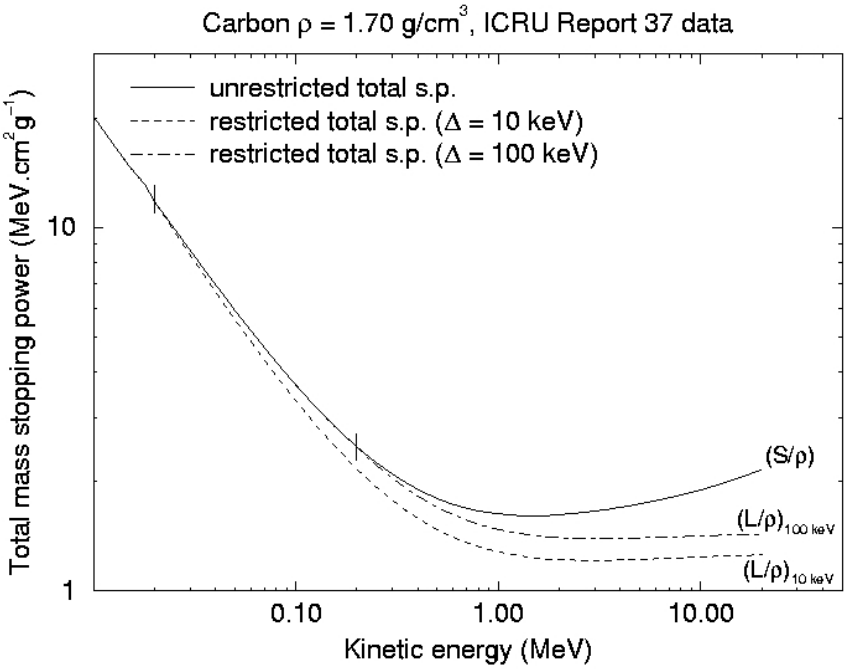

FIG. 7 Unrestricted S/ρ and restricted ((L_Δ/ρ) with Δ = 10 keV and 100 keV) total mass stopping powers for carbon, based on data published in the ICRU Report 37. Vertical lines indicate the points at which restricted and unrestricted mass stopping powers begin to diverge as the kinetic energy increases.

Relationships between fluence and dose (electrons)

Under the conditions that (1) radiative photons escape the volume of interest and (2) secondary electrons are absorbed on the spot (or there is charged particle equilibrium of secondary electrons), the absorbed dose to a medium D_{med} is related to the electron fluence Φ_{med} in the medium, as follows:

$$D = \Phi_{med}\left(\frac{S_{coll}}{\rho}\right)_{med} \qquad 6.3$$

where $\left(\frac{S_{coll}}{\rho}\right)_{med}$ is the *unrestricted mass collisional stopping power* of the medium at the energy of the electron.

Owing to electron slowing down in the medium, even for a mono-energetic starting electron of kinetic energy E_0 there is always a primary electron fluence spectrum in the medium denoted by $\Phi_{med,E}(E)$, which is differential in energy and ranges from E_0 down to zero. In this case, the absorbed dose to the medium can be obtained by an integration of Eq. 6.3:

$$D_{med} = \int_0^{E_0} \Phi_{med,E}(E)\left(\frac{S_{coll}(E)}{\rho}\right)_{med} dE = \Phi_{med}\left(\frac{\overline{S}_{coll}}{\rho}\right)_{med} \qquad 6.4$$

The right hand side of Eq. 6.4 shows that absorbed dose can be calculated using an equation formally similar to Eq. 6.3, by making use of spectrum-averaged collisional stopping power and total fluence.

The full, realistic electron fluence spectrum consists of primary charged particles that are, for example, the result of a multienergetic photon beam or electron beam interacting in the medium. These primary charged particles are slowed down and result in a secondary particle fluence. This fluence thus contains charged particles resulting from slowing down through soft collisions as well as delta electrons resulting from hard, knock-on collisions.

7: Cavity theory

The Bragg-Gray cavity theory

The Bragg-Gray cavity theory was the first cavity theory developed to provide a relationship between absorbed dose in a dosimeter and the absorbed dose in the medium containing the dosimeter.

The conditions for application of the Bragg-Gray cavity theory are:

1. the cavity must be *small when compared with the range of charged particles incident on it* so that its presence does not perturb the fluence of charged particles in the medium;
2. the absorbed dose in the cavity is deposited *solely by charged particles crossing it*, i.e., photon interactions in the cavity are assumed negligible and thus ignored.

The result of condition (1) is that the *electron fluences in Eq. 6.4 are the same and equal to the equilibrium fluence established in the surrounding medium*. This condition can only be valid in regions of CPE or TCPE. In addition, the presence of a cavity always causes some degree of fluence perturbation, which requires the introduction of a *fluence perturbation correction factor*.

Condition (2) implies that all electrons depositing the dose inside the cavity are produced outside the cavity and completely cross the cavity. Therefore, *no secondary electrons are produced inside the cavity and no electrons stop within the cavity*.

Under these two conditions, according to Bragg-Gray cavity theory, the dose to the medium D_{med} is related to the dose in the cavity D_{cav} as follows:

$$D_{med} = D_{cav}\left(\frac{\bar{S}}{\rho}\right)_{cav}^{med} \qquad 7.1$$

where $\left(\frac{\bar{S}}{\rho}\right)_{cav}^{med}$ is the ratio of the average unrestricted mass collisional stopping powers of the medium and cavity. The use of unrestricted stopping powers rules out the production of secondary high-energy charged particles (delta electrons) in the cavity and the medium.

The dose to the cavity gas D_{cav} is simply related to the ionization produced in the cavity by:

$$D_{cav} = \frac{Q}{m}\left(\frac{W}{e}\right)_{cav} \qquad 7.2$$

Here, it may be noted that W/e for air is 33.97 eV/ion pair, or 33.97 J/C.

The Spencer-Attix cavity theory

The Bragg-Gray cavity theory does not take into account the creation of secondary high-energy (delta) electrons generated as a result of the slowing down of the primary electrons via hard collisions in the sensitive volume of the dosimeter. The Spencer-Attix cavity theory is a more general formulation that accounts for the production of these electrons that themselves have sufficient energy to produce further ionisation. Some of these electrons released inside the cavity will have sufficient energy to escape from the cavity, carrying some of their energy with them. This reduces the energy absorbed in the cavity, and requires modification to the stopping power of the gas.

The Spencer-Attix cavity theory operates under the two Bragg-Gray conditions; however, these conditions now also apply to the secondary charged particle fluence, in addition to the primary charged particle fluence.

The secondary electron fluence in the Spencer-Attix theory is divided into two components based on the user-defined energy threshold Δ. Secondary electrons with kinetic energies E less than Δ are considered slow electrons that deposit their energy locally; secondary electrons with energies larger than or equal to Δ are considered fast (slowing down) electrons and are part of the electron slowing-down spectrum. Consequently, this spectrum has a low energy threshold of Δ and a high energy threshold of E_0. Hence, energy deposition is calculated as the product of $L_\Delta(E)/\rho$ (the restricted mass collisional stopping power with threshold Δ), and the fast electron fluence with electrons ranging in energy from Δ to E_0, $\Phi^{\delta}_{med,E}$, where the δ here indicates the inclusion of the contribution of the delta electrons in the slowing-down spectrum.

Because of the second Bragg-Gray condition which stipulates that there must not be electron production in the cavity, electrons with energy Δ must be capable of crossing the cavity. Hence, the threshold value Δ is related to the cavity size and is usually defined as the energy of an electron with range equal to the mean chord length across the cavity. (Usually for ion chamber problems, Δ is set at a nominal value of 10 keV.)

The Spencer-Attix relation between the dose to the medium D_{med} and the dose in the cavity D_{cav} is thus written as:

$$D_{med} = D_{cav}\left(\frac{\overline{L}_\Delta}{\rho}\right)^{med}_{cav} \qquad 7.3$$

where $\left(\frac{\overline{L}_\Delta}{\rho}\right)_{cav}^{med}$ is the ratio of the mean restricted mass collisional stopping power of the medium to that the cavity. (This may be compared to Eq. 7.1, which is the Bragg-Gray relation.)

Using the electron fluence spectrum in the medium $\Phi^{\delta}_{med,E}(E)$, the full expression is:

$$\left(\frac{\overline{L}_\Delta}{\rho}\right)_{cav}^{med} = \frac{\int_\Delta^{E_0} \Phi^{\delta}_{med,E}(E)\left(\frac{L_\Delta}{\rho}\right)_{med} dE + TE_{med}}{\int_\Delta^{E_0} \Phi^{\delta}_{med,E}(E)\left(\frac{L_\Delta}{\rho}\right)_{cav} dE + TE_{cav}} \qquad 7.4$$

The terms TE_{med} and TE_{cav} are track-end terms and account for the energy deposited by electrons with initial kinetic energies between Δ and 2Δ.

The track-end electrons have an energy loss that brings their kinetic energy to lower than Δ. Their residual energy after such events is therefore deposited on the spot, and these electrons are then removed from the spectrum. The track-end terms are approximated by Nahum as:

$$TE_{med} = \Phi^{\delta}_{med,E}(\Delta)\left(\frac{S_{coll}(\Delta)}{\rho}\right)_{med} \Delta \qquad 7.5$$

and

$$TE_{cav} = \Phi^{\delta}_{med,E}(\Delta)\left(\frac{S_{coll}(\Delta)}{\rho}\right)_{cav} \Delta \qquad 7.6$$

Note that the unrestricted collisional stopping powers are used here because the maximum energy transfer for an electron with energy less than 2Δ is less than $\tilde{\Delta}$.

Monte Carlo calculations show that the difference between the Spencer-Attix and Bragg-Gray cavity theories is non-negligible, yet generally not very significant. Since collisional stopping powers for different media show similar trends as a function of particle energy, their ratio for two media is a very slowly varying function with energy. (For ionisation chambers in water, the energy dependence arises mainly from the difference in the density effect correction between the two materials, water and air.)

Large cavity theory

Bragg-Gray and Spencer-Attix cavity theory is applied to the case of small cavities (ion chambers, other small dosimeters) in a medium. The fluence of charged particles in the cavity is largely unaffected by the presence of the cavity.

At the opposite extreme we have large cavities; a large cavity has dimensions such that the dose contribution from photon interactions outside the cavity may be ignored, compared with the contribution from electrons liberated by photon interactions inside the cavity.

Under these conditions there exists a condition of charged-particle equilibrium in the central regions of the cavity far from the walls. Given this, it is clear that (a) $D_{cav} = K_{coll}$ within the cavity (see Figure 6 and Eq. 5.1, 5.9), and that (b) $\Psi_{med} = \Psi_{cav}$.

In this case the ratio of dose between the medium and the cavity is clearly given simply by the ratio of the collisional kerma in the medium to that in the cavity, and from Eq. 5.5 is also equal to the ratio of the average mass-energy absorption coefficients,

$$\frac{D_{med}}{D_{cav}} = \frac{K_{coll,med}}{K_{coll,cav}} = \left(\frac{\overline{\mu}_{en}}{\rho} \right)_{cav}^{med} \qquad 7.7$$

This is used in the derivation of air-kerma standards, where the cavities used are quite large (Figure 3 for example).

8: Protection

Equivalent dose H_T

$$H_T = \sum w_R D_{T,R} \qquad 8.1$$

Where $D_{T,R}$ is the absorbed dose (averaged over a tissue or organ T) due to radiations of type R and w_R is the radiation weighting factor. $D_{T,R}$ can not be measured experimentally. The weighting factor is introduced to weight the absorbed dose for biological effectiveness of the particles.

Type and energy of radiation R	**Radiation weighting factor w_R**
Photons, all energies	1
Electrons and muons, all energies	1
Neutrons	
<10 keV	5
10 to 100 keV	10
> 0.1 to 2 MeV	20
> 2 to 20 MeV	10
> 20 MeV	5
Protons, other than recoil protons, >2 MeV	5
Alpha particles, fission fragments, heavy nuclei	20

Unit: J kg^{-1}

Special name for the unit of equivalent dose is sievert (Sv).

Effective dose E

$$E = \sum_T w_T H_T = \sum_T w_T \sum_R w_R D_{T,R} \qquad 8.2$$

where $D_{T,R}$ is as above and w_T is a tissue weighting factor which reflects the total detriment to health.

Tissue or organ	Tissue weighting factor w_T
Gonads	0.20
Bone marrow (red)	0.12
Colon	0.12
Lung	0.12
Stomach	0.12
Bladder	0.05
Breast	0.05
Liver	0.05
Oesophagus	0.05
Thyroid	0.05
Skin	0.01
Bone surface	0.01
Remainder	0.05
Whole body total	1.00

Unit: J kg^{-1}

Special name for the unit of effective dose is sievert (Sv).

Protection: Operational quantities

For measurement purposes the operational quantities: ambient dose equivalent and directional dose equivalent, are defined.

Ambient dose equivalent $H^*(d)$

The ambient dose equivalent $H^*(d)$, at a point, is the dose equivalent that would be produced by the corresponding expanded and aligned field, in the ICRU sphere at a depth d in millimetres on the radius opposing the direction of the aligned field. For measurement of strongly penetrating radiations the reference depth used is 10 mm and the quantity denoted $H^*(10)$

Unit: J kg^{-1}

Special name for the unit of ambient dose equivalent is sievert (Sv).

Directional dose equivalent $H'(d,\Omega)$

The directional dose equivalent $H'(d, \Omega)$, at a point, is the dose equivalent that would be produced by the corresponding expanded field in the ICRU sphere at a depth d on a radius in a specified direction Ω. Directional dose equivalent is of particular use in the assessment of dose to the skin or eye lens.

Unit: J kg^{-1}

Special name for the unit of directional dose equivalent is sievert (Sv).

References

1. Fundamentals of Radiation Dosimetry J R Greening, medical Physics handbook, No 15 2nd Edition 1985 Adam Hilger, Bristol
2. ICRU Report 60 Fundamental Quantities and Units for Ionising Radiation 1998 (http://www.icru.org/)
3. ICRP Report 60 1990 Recommendations of the International Commission on Radiological Protection (http://www.icrp.org/)
4. Bureau International des Poids et Mesures (BIPM). http://www.bipm.org/en/home/
5. National Physical Laboratory (NPL) http://www.npl.co.uk/npl/reference/
6. National Institute of Standards and Technology (NIST) http://physics.nist.gov/cuu/index.html
7. Health Protection Agency (HPA) http://www.hpa.org.uk/radiation/
8. Campion, P.J., 1959. The standardization of radioisotopes by the beta-gamma coincidence method using high efficiency detectors. Int. J. Appl. Radiat. Isot. (4) 232-248.
9. ICRU Report 52 1994 Particle Counting in Radioactivity Measurement
10. NPL Calorimetry: The evolution so far http://www.npl.co.uk/~ard/calws_99/index.htm
11. A R S Marsh, T T Williams. 50 kV Primary Standard of Exposure 1978 Design of Free-Air Chamber; NPL Report RS(EXT) 54; April 1982
12. BIR Working Party on SI Units. 1981 Conversion to SI units in radiology. British Journal of Radiology, (54) 377-380.
13. Radiation Oncology Physics: A Handbook for Teachers and Students. EB Podgorsak, Technical Editor; IAEA 2005 http://www-pub.iaea.org/MTCD/publications/PDF/Pub1196_web.pdf
14. F.H. Attix, “Introduction to Radiological Physics and Radiation Dosimetry”, John Wiley, New York, New York (1986).

Overview of Dosimetry

1. Introduction

It would seem self-evident that the meaning of dosimetry is the measurement of dose. In radiation measurement the only proper use of the term dose is as an abbreviation for absorbed dose. However, in a wider sense the term dosimetry is used to refer to measurement of various quantities related to the effects of radiation on matter: energy imparted per unit mass (absorbed dose), kinetic energy released per unit mass (kerma), numbers of particles (e.g. fluence) or a function of the above quantities such as the product of absorbed dose and a biological radiation quality factor.

Many different detectors have been developed for the measurement of ionising radiation. Its fundamental property, the ability to split neutral atoms and molecules into charged ions and free radicals is the cause of the harmful effects in biological systems on which radiotherapy depends. The amount of damage done is related to the energy absorbed from the radiation. It turns out that this relation is proportional for high-energy photon and electron beams.

The energy W required to create an ion pair is only of the order a few electron volts (the value depends on the material), but an electron with a kinetic energy of thousands or millions of electron volts will create a large number of ion pairs and do damage in proportion to their number. To a good approximation, W is independent of the energy of the primary radiation and takes the same value for high-energy photons and electrons.

At low intensities (doses), most of the immediate effects of ionising radiation on biological systems are reversed within a few hours by the highly effective repair mechanisms operating inside cells. What remains are random (stochastic) effects in which the probability of occurrence is proportional to the dose received.

This is the basis of the current view, which is that the most useful quantity for the measurement of ionising radiation is absorbed dose. Water has been chosen as the preferred absorber, because it is similar enough to tissue.

An overview is given of various detectors that are used for dosimetry with emphasis on those that are used for absolute or reference measurement of absorbed dose or air kerma and those that from the basis of primary standards. They can be devided in three categories: detectors that directly measure the quantity absorbed dose, detectors that measure ionisation and detectors that quantify in a direct or indirect way the number of radicals formed in a medium. The lecture ends with a brief discussion on the relation between the energy dependence of the detector response and the beam quality specification.

2. Detectors

2.1. Dosimeters directly measuring the energy imparted: calorimeters

A charge liberated in the medium by an energetic ionising particle results in an energy cascade in which the energy of the initial particle is shared among many less energetic secondary particles. Eventually charges and ions recombine and the liberated energy ends up as heat, which can be measured as a temperature rise. However, even though a typical radiotherapy treatment fraction creates enough ionisation in the target volume to cause cell death through biochemical processes, the amount of energy involved is tiny. The technique of deriving absorbed dose via a measurement of the temperature rise is called calorimetry.

The temperature rise in the calorimeter medium is proportional to absorbed dose according to the specific heat capacity of the absorbing medium under the condition that no physico-chemical changes of the state of the medium take place as a result of the irradiation. If such a change takes place the energy deficit is called the heat defect.

The expression to derive absorbed dose to the medium D_{med} from the measured temperature rise ΔT is

$$D_{med} = c_{med} \cdot \Delta T \cdot \frac{1}{1-h}$$

where c_{med} is the specific heat of the absorbing medium and h is the heat defect of the medium. The main challenges for calorimetry are the control of the heat defect and the prevention of heat exchange between the irradiated material and its environment. The heat defect of different materials has been measured by different authors and a review on this can be found in the ICRU report 64.

Material	ρ (kg m^{-3})	c (J kg^{-1} K^{-1})	k (J s^{-1} m^{-1} K^{-1})	α (m^2 s^{-1})	ΔT/D (mK Gy^{-1})
Water	998	4180	0.602	1.44×10^{-7}	0.24
Graphite	1770	725	135	1.05×10^{-4}	1.4

Table 1: Thermal properties of water and graphite: the mass density ρ, the specific heat capacity c, the thermal conductivity k and the thermal diffusivity α. The last column gives the temperature rise due to an absorbed dose of 1 Gy.

Table 1 gives some thermal properties of water and graphite as well as the temperature rise that is the result of an absorbed dose of 1 Gy. It is obvious that these temperature increases are very small and require sensitive technology for temperature measurement as well as excellent temperature control. Figure 1 gives a schematic overview of how calorimetry is implemented. The devices to measure the temperature rise are thermistors in contact with the calorimeter medium and coupled into a Wheatstone bridge.

The measurement typically involves the recording of temperature drift curves before and after the irradiation and extrapolations to mid-run to derive the ionising radiation induced temperature rise, although a variety of alternative operational and analysis techniques are in use.

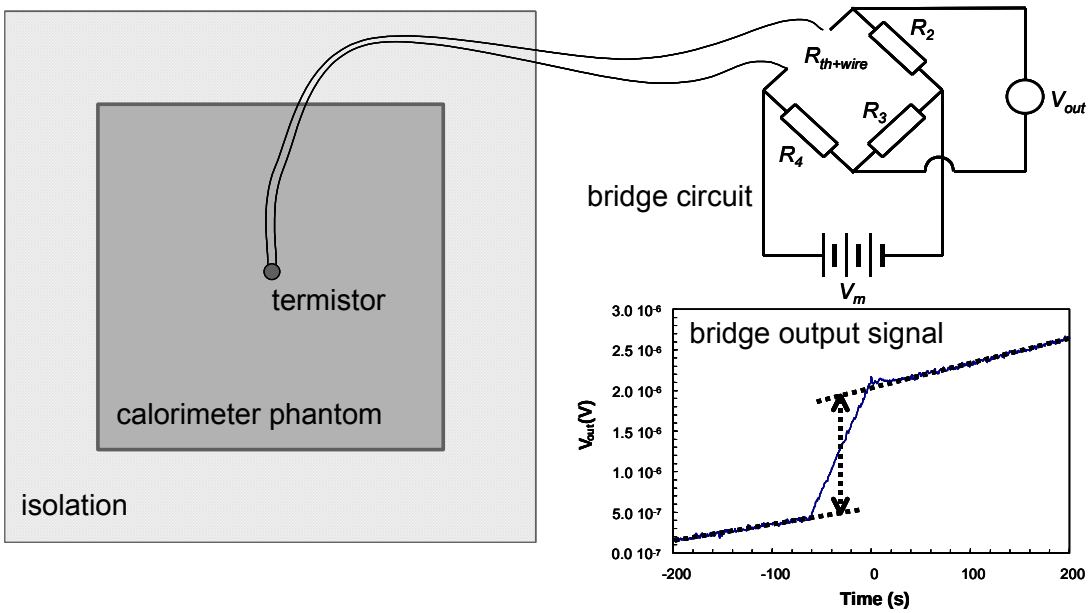

Figure 1: Schematic representation of a calorimeter set-up including a calorimeter phantom, thermally isolated from its environment, a thermistor coupled into a Wheatstone bridge and a typical bridge output signal.

2.1.1. Graphite calorimeters

Table 1 shows that for the same dose, the temperature rise in graphite will be six times the temperature rise in water. This puts less stringent requirements on the sensitivity of the temperature probe and is one of the reasons why graphite calorimetry as a dosimetry technique has been developed much earlier than water calorimetry. NPL's absorbed dose standards are at present based on graphite calorimeters.

In graphite calorimetry, lattice impurities and chemical reactions with dissolved oxygen have been proposed as mechanisms for a potential heat defect, but they are in general assumed to be negligible. Experiments have confirmed this within the achievable uncertainties.

As can be seen from table 1, the thermal diffusivity in graphite is much larger than in water and its magnitude is such that heat deposited in a graphite volume distributes itself within that volume in a timescale of milliseconds, far too short to allow an accurate measurement of temperature rise at the point of measurement inside the phantom. Hence, in graphite calorimeters a core needs to be thermally isolated from the surrounding graphite by one or more air or vacuum gaps as shown in figure 1.

Since we use graphite calorimeters, the primary standards do not, after all, quite realise the quantity that we disseminate in our calibration services. For both photon and electron beams, we maintain sets of reference standard

ionisation chambers which are calibrated in terms of absorbed dose to graphite by direct comparison against the relevant primary standard. By a combination of theoretical analysis, experimental measurement and Monte Carlo simulation, the calibrations of these chambers are converted from dose to graphite to dose to water. These reference chambers are then used, in water, to calibrate our own and other secondary standard chambers.

The conversion to water introduces several factors, of which the most significant are the ratios of photon mass-energy absorption coefficients (for photon beams) and electron mass stopping powers (for electron beams), for water and graphite. These are reasonably well known (i.e. with only small uncertainty), and vary by less than 1.5% over the range of energies available from the NPL linac.

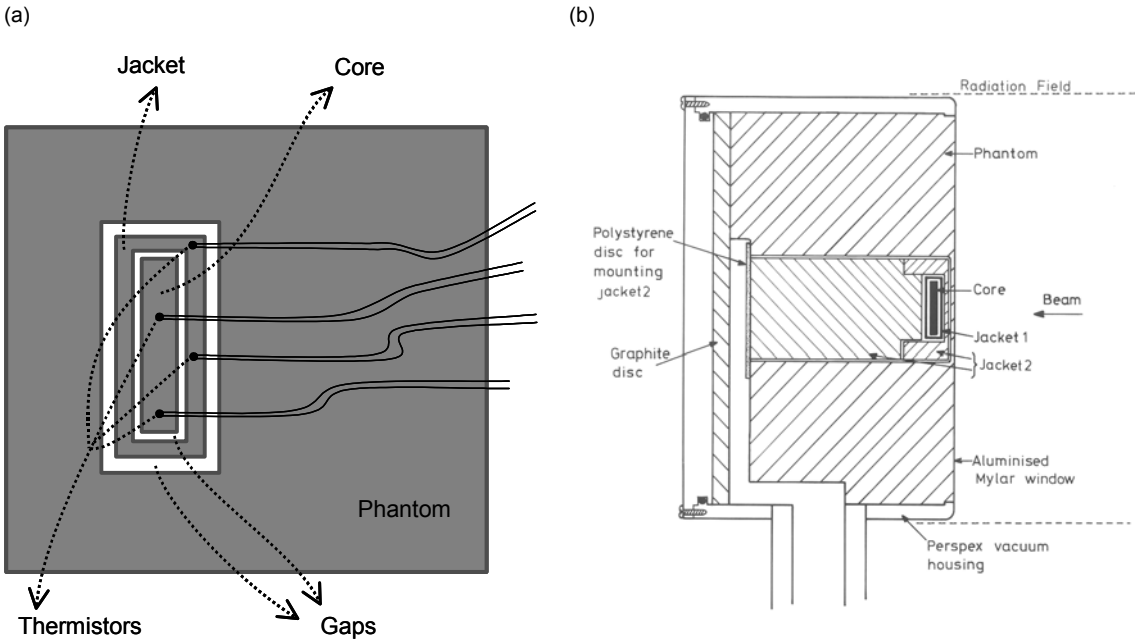

Figure 2: (a) Schematic drawing of a simplified graphite calorimeter and (b) sketch of the graphite calorimeter that forms the basis of NPL's primary absorbed dose to water standard for high-energy photon beams.

Overall, the variation of the correction factors that apply to the primary standard calorimeters is less than 1 %. They also take account of:

- The effect of gaps in the nearly homogeneous graphite calorimeter
- Beam uniformity effects due to the finite size of the calorimeter core

2.1.2. Water calorimeters

Water calorimeters have been developed since about 1980, when Domen (1980) realized that it is not required to thermally isolate a sample of water to measure the dose. Due to the low heat diffusivity of water, the spatial dose

distribution due to the irradiation remains stable for a period of time, which is long enough to allow an accurate measurement of the temperature rise. For water calorimetry, correction factors have to be applied to the basic calorimetry equation for scatter perturbations, conductive heat flows, convective heat flows, non-uniformity of dose distributions and radiation induced chemical reactions.

For water calorimetry, a chemical heat defect results from the chemical reactions that take place between radiation induced radicals and chemicals in the aqueous environment. Especially when impurities are present these reactions can result in net endothermic or exothermic effects. The measured heating of the medium is then not equal to the energy that has been dissipated locally by radiation. The proper control of the chemical heat defect requires the use of very high purity water and good control of solved gasses.

Water calorimetry should, in principle, be regarded as the preferred method for reference dosimetry as it is the most direct way to determine the quantity of interest, absorbed dose-to-water. However, it is a time consuming method and not very suitable for periodic dosimetry in a clinical environment.

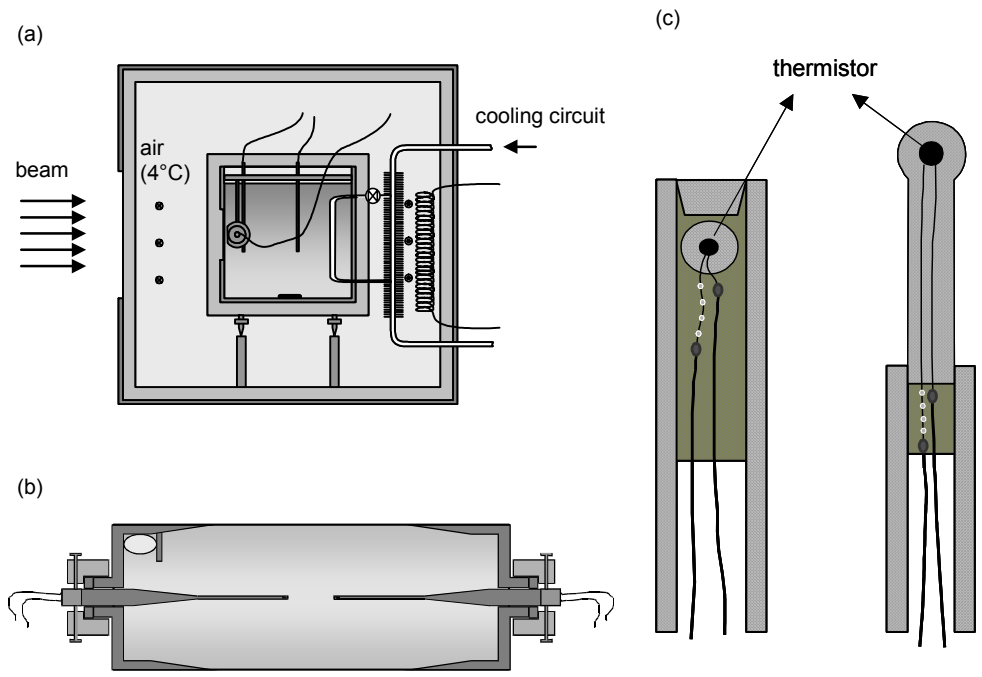

Figure 3: (a) Sealed water calorimeter phantom with is enclosure, (b) cylindrical glass vessel with thermistor probes positioned and (c) detail of the thermistor probes.

2.2. Dosimeters measuring ionisation

Ionisation is the physical process at the heart of most precise measurements in dosimetry though the ionisation is not in a biological system, but usually in air. An electric field is applied to the sensitive volume, which sweeps the ionisation onto electrodes of opposite polarity. The electric current produced is

usually tiny (a fraction of a nanoamp) but it is at least an order of magnitude easier to measure this than to measure the millidegree temperature rise in our calorimeters.

The amount of ionisation is proportional to the mass of the sensitive volume – when this is air at ambient pressure, account must be taken of density variations, by correcting to standard temperature and pressure.

So in principle we can derive dose to air D_{air} in the cavity from the charge Q_{air} collected on the collecting electrode from the accurate knowledge of the volume, the air density ρ_{air} and the fundamental quantity W_{air}, which is the mean energy required to produce an ion pair in dry air (W_{air} = 33.97 eV for radiotherapeutic photon and electron beams).

$$D_{air} = \frac{Q_{air}}{\rho_{air} \cdot V} \cdot \frac{W_{air}}{e}$$

Note that if the air density ρ_{air} in this expression refers to normal conditions of pressure and temperature, the charge should be corrected for any deviation from normal conditions at the time and location of the measurement, using the temperature and pressure correction factor

$$f_{pT} = \frac{1013.25}{p} \cdot \frac{(T + 273.15)}{293.15}$$

If it is an air volume surrounded by a medium then Bragg-Gray cavity theory is used to relate absorbed dose to air in the cavity to absorbed dose in the medium:

$$D_{med} = D_{air} \cdot \left(\frac{S^{SA}}{\rho} \right)_{med,air}$$

where $(S^{SA}/\rho)_{med,air}$ is the medium to air Spencer-Attix stopping power ratio for the charged particle fluence spectrum present in the undisturbed medium.

The ionisation in air depends weakly on the relative humidity (RH), but this variation is negligible (less than 0.1%) provided RH lies between 20% and 70%.

Finally, some positive and negative ions may recombine before they reach the electrodes: the smaller the electric field applied, the slower the ions drift, and the more time they have to recombine. Recombination also increases with ion density and hence with (instantaneous) dose rate. For this reason, pulsed beams show greater and variable amounts of recombination, and care must be taken when transferring a calibration between one pulsed beam and another, or between a continuous and a pulsed beam.

2.2.1. Free-air ionisation chambers

A direct measurement of the kinetic energy released by photons interacting in air is unfortunately not possible. Instead, we collect the ionisation produced as this kinetic energy is spent breaking up the atoms in air. The quantity

exposure (total charge of one sign produced per unit mass of air) is much more closely related to free-air chamber operation. The required conversion from exposure to air kerma introduces more factors, of which the energy required to produce an ion pair in dry air, W_{air}, is the key ingredient.

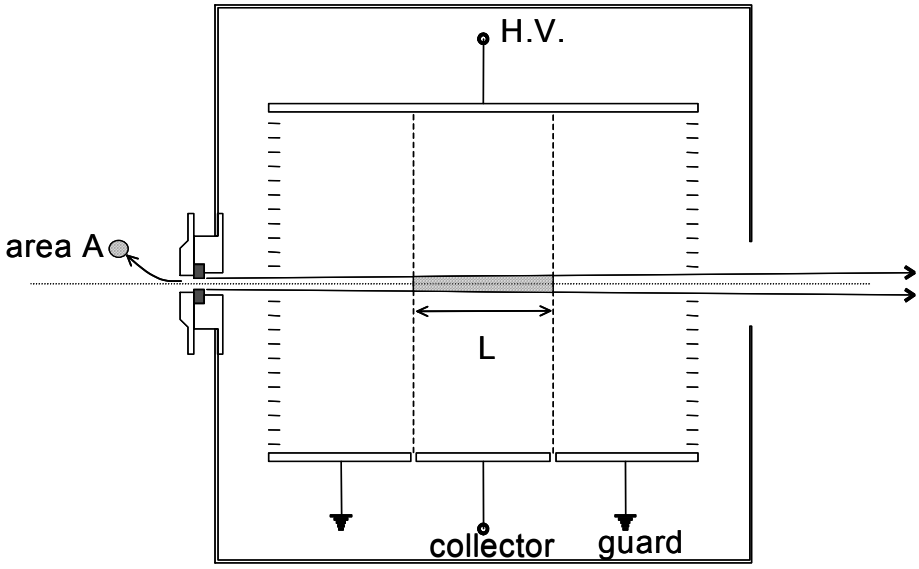

Figure 4: Schematic representation of a free air ionisation chamber.

The key to understanding the principle of a free-air chamber design is the idea of charged particle (electron) equilibrium, CPE. Every photon passing through the aperture at the front of the chamber goes on to interact at some point downstream. The chamber must be large enough that, if the interaction occurs in the plane of the aperture, the resulting electron cannot reach the collecting volume. In that case, every electron which does reach the collecting volume must have originated somewhere inside the air volume enclosed by the chamber. Neglecting the effects of photon attenuation, and considering all possible electron tracks, one can see that for every electron track leaving one end of the collecting volume, there will be another track entering the collecting volume at the opposite end. A reciprocity theorem states that the total length of those parts of all electron tracks that lie within the collecting volume is the same as the total length of the complete tracks of only those electrons that start in the collecting volume.

In this way we can relate the quantity of interest (kerma) which is associated with the point at which photons first interact, to the quantity that the free-air chamber responds to (ionisation) which is associated with the points at which the photons' energy is finally absorbed.

The sensitive volume V of a free-air chamber is the product of the aperture area A and the effective length L of the collecting volume (see figure 4)

Apart from the factors required to convert exposure into air kerma, the corrections applied to the free-air chamber reading take account of:

- Attenuation of the primary X-ray beam between the aperture and the collecting volume (K_{att})

- The extra ionisation collected from electrons produced by photons scattered within the chamber (K_{sc})
- Ionisation lost when electrons strike the collecting electrode (non-zero only when the free-air chamber is smaller than optimal) (K_e)

The overall expression to derive air kerma from the measured charge Q_{air} becomes

$$K_{air} = \frac{Q_{air}}{\rho_{air} \cdot V} \cdot \frac{(W_{air}/e)}{(1-g)} \cdot K_{att} \cdot K_e \cdot K_{sc} \cdot K_{hum} \cdot K_{pol} \cdot K_{ion}$$

where, besides the quantities defined above, g is the fraction of kinetic energy of charged particles that is lost in radiative energy (such as bremsstrahlung), and K_{hum} the humidity correction factor, K_{pol} the correction for the difference between the charge measured when operating at polarising voltages that are equal in magnitude but opposite in sign and K_{ion} the correction factor for ionisation losses due to recombination.

2.2.2. Cavity ionisation chambers

The size of a free-air chamber should be twice the range of the maximum energy electron generated by the photon beam being measured. For ^{60}Co γ-radiation, this would be several metres, and quite impractical. Even if the chamber were operated at elevated air pressure, the attenuation and scatter corrections would be uncomfortably large. Instead, standards laboratories have adopted graphite-walled cavity chambers (graphite is reasonably air-equivalent) in which the sensitive volume can be measured mechanically. These chambers are mostly intended to realise air kerma (originally exposure). The steps required to derive air kerma from the measured charge are explained below and are illustrated in figure 5.

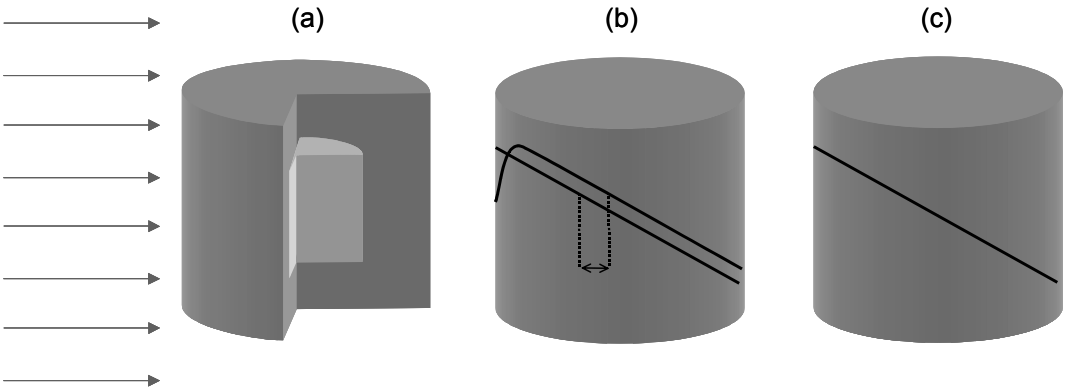

Figure 5: Steps in the derivation of air kerma free in air from the ionisation in a graphite walled cavity ionisation chamber.

As seen before, dose to air for the electron fluence spectrum present in the air cavity can be derived provided the volume of the cavity is accurately known:

$$D_{air} = \frac{Q_{air}}{\rho_{air} \cdot V} \cdot \frac{W_{air}}{e}$$

Applying Bragg-Gray cavity theory using Spencer-Attix stopping power ratios yields absorbed dose in graphite (figure 5a):

$$D_g = D_{air} \cdot \left(\frac{S^{SA}}{\rho} \right)_{g,air}$$

Absorbed dose in graphite equals collision kerma in graphite apart from a displacement due to the finite range of the electrons produced in graphite (figure 5b). This can be accounted for by a correction factor K_{cep}:

$$K_{col,g} = D_g \cdot K_{cep}$$

Collision kerma in graphite is related to collision kerma in the surrounding air through the ratio of mass energy absorption coefficients. Correction factors for attenuation and scatter in the wall thickness need to be applied (figure 5c):

$$K_{col,air} = K_{col,g} \cdot \left(\frac{\mu_{en}}{\rho} \right)_{air,g} \cdot K_{att} \cdot K_{sc}$$

Correction for radiative losses yields kerma in air:

$$K_{air} = \frac{K_{col,air}}{(1-g)}$$

The overall expression becomes

$$K_{air} = \frac{Q_{air}}{\rho_{air} \cdot V} \cdot \frac{(W_{air}/e)}{(1-g)} \cdot \left(\frac{S^{SA}}{\rho} \right)_{g,air} \cdot \left(\frac{\mu_{en}}{\rho} \right)_{air,g} \cdot \prod K_i$$

where

$$\prod K_i = K_{att} \cdot K_{cep} \cdot K_{sc} \cdot K_{stem} \cdot K_{hum} \cdot K_{pol} \cdot K_{ion}$$

The product $K_{att} \cdot K_{sc} \cdot K_{cep}$ is summarised as K_{wall}. In the past, there has been considerable debate about this factor since part of it, $K_{att} \cdot K_{sc}$, used to be measured in many PSDLS by a linear extrapolation method, which has been proven to be wrong. Other PSDL's, including NPL, based wall perturbation correction factor on a full Monte Carlo simulation of the response of the ionisation chamber. It is now generally accepted that K_{wall} should be obtained from such a simulation.

One correction factor that has not been mentioned before is K_{stem}, which corrects for the perturbation of the radiation field due to the stem. It is usually measured by putting a dummy stem on top of the chamber.

NPL maintains a set of three primary standard cavity ionisation chambers, which are now over 40 years old, and their replacement with new chambers is ongoing in the present programme.

It is also possible to realise absorbed dose to water using an ionisation chamber. This is the procedure adopted by the BIPM and their standard is (arbitrarily) selected to provide the reference value in the worldwide key comparison database for absorbed dose to water. The method also requires the ratio of photon mass-energy absorption coefficients water to graphite, the ratio of electron mass-stopping powers graphite to air, the W_{air} value, the fraction of energy, g, going into bremsstrahlung and correction factors for photon scatter and attenuation in the chamber wall. The steps required in this procedure are illustrated in figure 6.

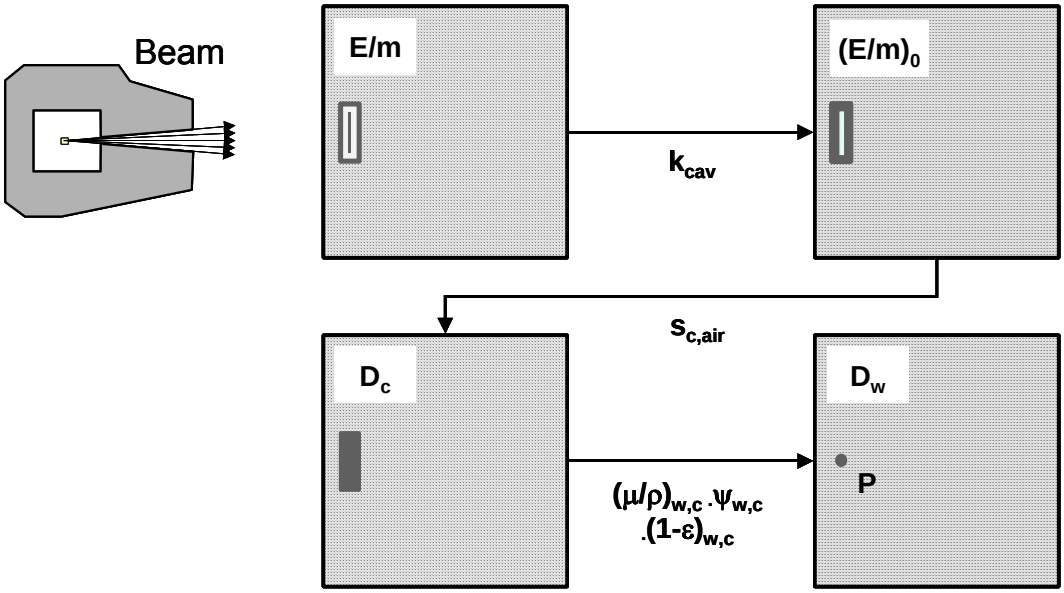

Figure 6: The successive steps considered in the derivation of absorbed dose to water air from the ionisation in a graphite walled cavity ionisation chamber positioned in a water phantom.

2.2.3. Extrapolation chambers

Extrapolation chambers are plane-parallel chambers of which the distance between the electrodes can be varied and accurately set. This allows one to derive the gradient of the ionisation with respect to the volume (proportional to the plate separation) and thus to avoid the need of calibrating the chamber as a means to determine its volume. Extrapolation chambers are

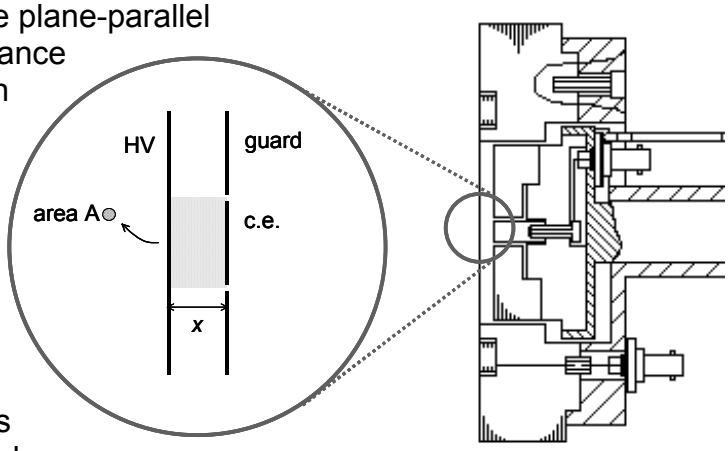

the basis of standards of absorbed dose in low and medium-energy x-rays as well as for beta emitting sources.

In an extrapolation chamber, not the charge per unit volume is measured, but the change of the measured charge when the volume is changed:

$$\begin{aligned} D_{air} &= \frac{Q_{air}}{\rho_{air} \cdot V} \cdot \frac{W_{air}}{e} \\ &= \frac{1}{\rho_{air}} \cdot \frac{dQ_{air}}{dV} \cdot \frac{W_{air}}{e} \\ &= \frac{1}{\rho_{air} \cdot A} \cdot \frac{dQ_{air}}{dx} \cdot \frac{W_{air}}{e} \end{aligned}$$

2.2.4. Ionisation in solid state detectors

Ionisation in solid semiconductors (diodes, diamond, germanium) provides the basis of extremely sensitive detectors which can either be made very small or which can count individual ionising particles with high efficiency. A disadvantage of this type of detectors is that they often exhibit a significant dose rate dependence.

In a TLD crystal, on the other hand, the free electrons created by radiation become trapped in a long-lived metastable state, and the dose received is inferred from the light given off when the crystal is subsequently annealed by heating. On the other hand, TLD shows a much more marked energy-dependence in its sensitivity when calibrated in terms of absorbed dose.

Solid-state detectors are usually not deemed to be appropriate for reference dosimetry but are commonly used as relative dosimeters.

2.3. Dosimeters measuring radical formation

Some radiation detectors make use of the fact that ionisation can leave radicals in the medium for a short or longer time, which can be quantified by direct or indirect methods.

2.3.1. Direct measurement of radical formation: ESR

In the case that permanent radicals are formed, the spin of the unpaired electron can be separated in two quantum mechanical energy states in a magnetic field. Excitation of these states shows a resonance at a certain radio frequency and an energy absorption spectrum can be measured around this resonance frequency. Figure 8 gives a schematic representation of this process.

Alanine, an amino acid, in crystalline form has this property of forming a stable radical and is used at NPL for dosimetry. One reason for interest in

alanine ESR is that the dosimeter readout is a non-destructive process, and the dosimeter may be kept for some years as an archival record of the dose actually delivered.

Over the whole range of megavoltage X-ray beam energies available at NPL, the alanine ESR signal really is proportional to the absorbed dose to water where the dosimeter was irradiated (the variation of alanine sensitivity with X-ray energy is within the range ± 0.5 %, and apparently random).

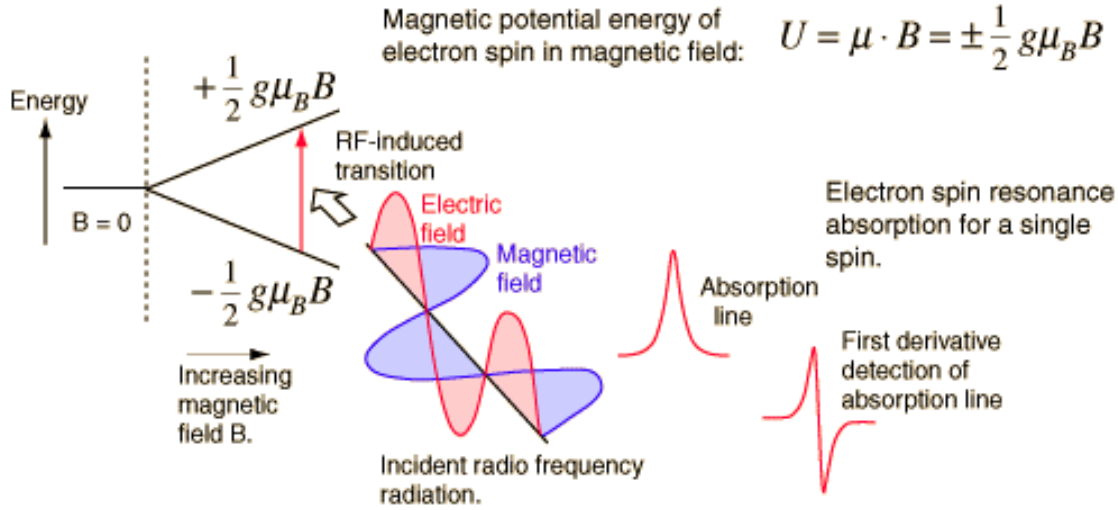

Figure 8: Concept of the measurement of the electron spin resonance signal of the alanine dosimeter.

2.3.2. Indirect measurement of radical formation: chemical dosimetry

In chemical dosimetry systems the dose is determined by measuring the chemical yield produced in the medium of the dosimeter due to irradiation. Various chemical systems are used but for standard dosimetry purposes the most commonly used chemical dosimeter is the ferrous sulphate dosimeter in which the change in optical absorbance due to the oxidation of Fe^{2+} ions to Fe^{3+} is measured with a spectrophotometer making use of the strong absorption peak of the latter ions at λ = 304 nm. The ferrous sulphate dosimeter response is expressed in terms of its sensitivity, known as the radiation chemical yield, G-value, and defined as the number of moles of ferric ions produced per joule of the energy absorbed in the solution. An advantage of this chemical dosimeter is that it is almost water equivalent.

In the use of the ferrous sulphate dosimeter as a primary standard, its sensitivity is determined by a total absorption experiment in which a known amount of charged particles with a known energy are totally absorbed in the ferrous sulphate solution. From this experiment the chemical yield is derived after correction for bremsstrahlung losses and scatter perturbation. The solution is then used in small quartz vials to determine dose to water in a water phantom, requiring a conversion from dose to ferrous sulphate solution and corrections for perturbations of the radiation field by the quartz walls of the vial.

Until recently it was assumed that the chemical yield of the ferrous sulphate dosimeter does not change with energy for high-energy photon and electron beams, but it has been shown that there is a variation of about 0.7% between 7the chemical yield in ^{60}Co and in high-energy photon beams

Chemical dosimetry could in principle be used as a primary method for the measurement of absorbed dose provided that the chemical yields (amount of molecules formed per 100 eV of absorbed energy) of the reactive species in the system are known. In practice this is not the case but the ferrous sulphate dosimeter has been used as a standard for establishing absorbed dose to water by totally absorbing an electron beam with known energy and integrated charge in the solution.

Other detectors that make use of the indirect results that radicals have in the chemical environment are radiographic film and gel dosimeters.

3. Energy dependence of dosimeters and beam quality

Many detectors for ionising radiation show an energy dependence of one or more response characteristics. It is therefore important to characterise this energy dependence and in addition, to be able to uniquely specify the complex energy spectrum of radiotherapeutic beams in an appropriate way.

For example, air-filled ionisation chambers used in megavoltage beams show a variation in sensitivity of a few per cent. The requirement is simple enough – to find a parameter QI (quality index) which is reasonably easy to measure, and which can be used to provide an unambiguous calibration curve, when the calibration is plotted against QI.

For megavoltage photons, this parameter is the Tissue Phantom Ratio ($TPR_{20/10}$) obtained as the ratio of ionisation currents at depths 10 and 20 cm from the front face of a water phantom, for a fixed source to chamber distance, and a fixed 10 × 10 cm field at the chamber. This parameter is not strongly sensitive to the actual source to chamber distance, but 1m is the conventional distance to use. Actually the use of $TPR_{20/10}$ as a beam quality index leaves some small ambiguity in the calibration factor, which has been observed at NPL to be at most 0.5%, but $TPR_{20/10}$ takes account of over 80 % of the variation with energy that is seen in the calibration factors of graphite-walled air-filled ion chambers.

For high-energy electrons, the beam quality parameter is essentially the range R_{50} at which the dose has fallen to 50 % of its peak value.

For medium energy X-rays, the calibration data are provided as a function of the half-value layer thickness (HVL) in aluminium

References

Three textbooks cover radiation dosimetry for radiotherapy:

Johns, H E and Cunningham, J R (1983) *The Physics of Radiology*, Charles C Thomas, Springfield IL, USA.

Evaluation of Uncertainties

My aim in these notes is to help you take account of errors and uncertainties in reporting the measurements you make, whether during calibrations, audits, or even in simple consistency checks. The essential ideas are introduced in a series of worked examples.

Errors vs. uncertainties

What we actually measure is not usually what we would like, or even intend. The difference between the result of a measurement and the right answer is the *error* – a discrepancy, rather than a mistake. Unfortunately, we never know exactly how large this error is. Instead we have to estimate this unknown error, and the outcome of this estimation is a statement of the measurement *uncertainty*:

A statement of uncertainty indicates how large the measurement error might be.

For instance, we could say that

$$T = T_m \pm U_T \tag{1}$$

where T is the true value, T_m is the measured value and $\pm U_T$ is the uncertainty. We mean that T probably lies in the range between $T_m - U_T$ and $T_m + U_T$, but to make this more precise, we must say what that probability is.

Example 1 – confidence limits

The ambient air pressure is measured with a barometer, and found to be 102.30 kPa. This result might be reported either as

102.30 ± 0.10 kPa, with 99% confidence limits (2)

or

102.30 ± 0.07 kPa, with 95% confidence limits. (3)

These are two different ways or reporting the *same* measurement: we have greater confidence in a measured value when it is quoted with a large uncertainty, and less confidence when the same value is quoted with a smaller uncertainty. We should decide, first, with what confidence probability the measurement result should be stated, and then work out what size interval will achieve this. The point of this example is to emphasise that an uncertainty statement is incomplete (meaningless!) unless that probability is specified.

Types of uncertainty

One direct way to obtain probabilities is from a statistical analysis. In repeated measurements, there will generally be some unintended or uncontrolled change in the conditions, so that the outcome of the measurement changes. We would take the mean result as the best estimate of the underlying (true) value and, with enough data, might interpret the standard deviation of the results as giving an indication of the uncertainty.

Example 2 – statistical analysis of uncertainty

It turns out that the previous example was the result of 10 readings taken over a short period of time:

p_i = 102.26, 102.26, 102.31, 102.41, 102.33,
102.32, 102.13, 102.45, 102.35, 102.21 kPa

Their mean was calculated using the formula

$$\overline{p} = \frac{1}{10}\sum_{i=1}^{10} p_i$$

and the result 102.303 kPa was rounded to two decimal places in the reported result. The standard deviation is obtained from

$$s(p) = \sqrt{\frac{1}{10-1}\sum_{i=1}^{10}\left(p_i - \overline{p}\right)^2} \tag{4}$$

and turns out to be 0.09 kPa.

If we repeated this several times, we would generate a series of mean values for the air pressure, and these mean values would themselves show a small random variation. We can estimate the standard deviation of these mean values, referred to as the standard uncertainty of the mean, using the formula

$$u_p = \frac{1}{\sqrt{10}}s(p)\,. \tag{5}$$

If enough readings are taken per mean value, then the distribution of mean values will be roughly gaussian, and the standard uncertainty corresponds to a confidence probability of 68%. We shall come back later to the question of how to obtain limits for other confidence probabilities such as those quoted above. The point of this example is to provide a gentle reminder of some key formulae.

Errors and uncertainties revisited

Individual readings in the second example can be written in terms of deviations from their mean value:

$$p_i = \overline{p} + \delta p_i$$

and then the standard deviation reduces to

$$s(p) = s(\delta p) = \sqrt{\frac{1}{10-1}\sum_{i=1}^{10}(\delta p_i)^2}\,.$$

This is an estimate of the standard deviation σ of the distribution from which the readings are taken. Each deviation δp_i may be thought of as the "error" of that reading, and the uncertainty of the mean is based on the statistics of these errors.

An uncertainty estimate derived like this, by a statistical analysis, is referred to as a Type A component of uncertainty; any other estimate is of Type B, which we consider below. This terminology was introduced in the ISO Guide to the Expression of Uncertainty in Measurement, or GUM. The type A estimate is only a *component* of uncertainty, because we must allow for the possibility that the result of our procedure is influenced by other sources of uncertainty that may affect all readings in the same way, as in the next example.

Example 3 – calibration uncertainty

Our pressure measurement is made, of course, with a barometer that has a traceable calibration. The certificate reports this calibration as a correction of 0.20 ± 0.10 kPa, for a coverage factor k = 2, with a confidence probability of 95%.

This calibration uncertainty contributes directly to the uncertainty in our pressure measurement. The calibration affects all measurements in the same way and so this component of uncertainty does not tend to cancel in repeated measurements, and will not show up in a statistical analysis. It is a Type B uncertainty component.

An additive correction Δ_p to the raw pressure reading p_{raw} can easily be recast as a multiplicative factor N_p:

$$p = p_{raw} + \Delta_p = p_{raw}\left(1 + \frac{\Delta_p}{p_{raw}}\right) \equiv p_{raw} N_p \,.$$

In this example, the calibration factor N_p is 1.0020.

It is not uncommon, as here, for a calibration certificate to quote the uncertainty with a higher degree of confidence than is represented by the standard uncertainty u. Such an *expanded uncertainty U* for an elevated confidence level is obtained by multiplying the standard uncertainty by a coverage factor, k, and we can recover the standard uncertainty on dividing by k:

$$u = \frac{U}{k}$$

In this example, the standard uncertainty is 0.05 kPa. Used in this way, k is also referred to as a reducing factor.

Example 4 – resolution uncertainty

Air temperature is measured with a mercury-in-glass thermometer having 0.2 °C graduations. Five readings are taken over a short period. The results, after applying the thermometer calibration correction, are:

T_i = 23.4, 23.4, 23.4, 23.4, 23.4 °C.

In this case the statistics are trivial: the mean value is $\overline{T} = 23.4\,°\text{C}$, and the standard deviation *s(T)* vanishes. Does this mean that the temperature uncertainty is zero? Of course not! Only the Type A component of uncertainty is zero.

Thinking further we realise that, because the thermometer only has a resolution of 0.2 °C, all we can say is that the temperature definitely lies somewhere in the range 23.3 to 23.5 °C. So we could report the measured temperature as

T = 23.4 ± 0.1 °C,

with 100% confidence. Since we arrived at this uncertainty by non-statistical reasoning, it must be another Type B uncertainty.

The point of this example is to highlight the fact that, even if the Type A uncertainty component vanishes, there will always be a Type B contribution coming from somewhere, whether a calibration factor, or the effect of limited resolution. In fact we must make Type B estimates for all sources of uncertainty, and can make Type A estimates only where repetition allows the statistical approach.

Indirect measurements

So far, the examples have been simple, in that the quantities of interest, air pressure and temperature, are directly accessible to measurement. More often, we are interested in a quantity that is accessible indirectly, and which must be inferred from the results of other measurements. Similarly, the uncertainty must be derived from the uncertainties of those other measurements.

Example 5 – measuring air density

The air pressure and temperature measurements in the examples so far are really only a means to an end, which is the determination of an air density correction k_{TP} for an ionisation measurement. Ionisation is proportional to air density, and the correction we need is the ratio of the air density under standard conditions (i.e. a pressure 101.325 kPa and a temperature 20 °C) divided by the density of the air in the collecting volume of the ion chamber at the time of the ionisation measurement:

$$k_{TP} = \frac{101.325}{p}\frac{(273.15+T)}{293.15}$$

in which the pressure p is in kPa, the temperature T is in °C, and both include calibration corrections. Using the data given in the examples above, this correction turns out to have a value 1.0020, but now we seek its uncertainty.

The formula for k_{TP} represents a model for our measurement of the air density correction. In any indirect measurement, such a model is an essential first step in the estimation of uncertainty. It arises from an analysis of the process

by which the measurement is made, and it makes explicit the consequences of our assumptions. In this case, we assume that the ideal gas law holds for the ambient air.

We begin by expressing the "true" values of temperature and pressure in terms of measured values and measurement errors:

$$p = p_m + \delta p$$
$$T = T_m + \delta T$$

The uncertainties of the measured pressure and temperature given earlier indicate how large the errors here might be. We seek an expression for the "true" value of the air density correction

$$k_{TP} = k_{TP,m} + \delta k_{TP} = k_{TP,m}\left(1 + \frac{\delta k_{TP}}{k_{TP,m}}\right)$$

written here as the sum of its measured value and error, in which the dependence on the measured temperature and pressure, and on *their* errors, must be made explicit.

The first step is to insert our expressions for the "true" temperature and pressure into the model equation for the air density correction:

$$\begin{aligned} k_{TP} &= \frac{101.325}{p_m + \delta p}\,\frac{(273.15 + T_m + \delta T)}{293.15} \\ &= \frac{101.325}{p_m}\left(1 + \frac{\delta p}{p_m}\right)^{-1}\left(\frac{273.15 + T_m}{293.15}\right)\left(1 + \frac{\delta T}{273.15 + T_m}\right) \\ &= k_{TP,m}\left(1 + \frac{\delta p}{p_m}\right)^{-1}\left(1 + \frac{\delta T}{273.15 + T_m}\right) \end{aligned}$$

in this last equation, the measured value of the correction, $k_{TP,m}$, is defined by inserting measured values of temperature and pressure into the model equation.

We assume that the measurement errors are all small and make the following first order approximations:

$$\left(1 + \frac{\delta p}{p_m}\right)^{-1} = 1 - \frac{\delta p}{p_m} + O(\delta^2)$$

and

$$\left(1-\frac{\delta p}{p_m}\right)\left(1+\frac{\delta T}{273.15+T_m}\right)=1-\frac{\delta p}{p_m}+\frac{\delta T}{273.15+T_m}+O(\delta^2)$$

so that the air density correction can be written

$$k_{TP}=k_{TP,m}\left(1-\frac{\delta p}{p_m}+\frac{\delta T}{273.15+T_m}\right)$$

and, in terms of the measured value and its error, we have

$$\frac{\delta k_{TP}}{k_{TP,m}}=-\frac{\delta p}{p_m}+\frac{\delta T}{273.15+T_m}\,.$$

The uncertainty is obtained as the standard deviation of this error. Square this expression and average, to get

$$\frac{\overline{\delta k_{TP}{}^2}}{k_{TP,m}{}^2}=\frac{\overline{\delta p^2}}{p_m{}^2}+\frac{\overline{\delta T^2}}{(273.15+T_m)^2}-\frac{2\,\overline{\delta p\,\delta T}}{p_m(273.15+T_m)}\,.$$

If the errors in pressure and temperature are uncorrelated, then the last term will vanish, giving:

$$\frac{s(\delta k_{TP})}{k_{TP,m}}=\sqrt{\frac{s(\delta p)^2}{p_m{}^2}+\frac{s(\delta T)^2}{(273.15+T_m)^2}}$$

Finally, we can write this in terms of the standard uncertainties, *u*:

$$\frac{u_{k_{TP}}}{k_{TP,m}}=\sqrt{\frac{u_p{}^2}{p_m{}^2}+\frac{u_T{}^2}{(273.15+T_m)^2}}\,.$$

Success! We have written the standard uncertainty of the air density correction as a weighted sum, in quadrature, of uncertainty components.

Sensitivity coefficients

It is often convenient to present the component uncertainties relative to measured values. Our equation is already in this form for the pressure, and would be for the temperature as well, if we had measured it in degrees kelvin, K, from the start. This is not essential, though, and we can persist with degrees celsius if we write the uncertainty in the form:

$$\frac{u_{k_{TP}}}{k_{TP,m}}=\sqrt{\frac{u_p{}^2}{p_m{}^2}+\frac{T_m{}^2}{(273.15+T_m)^2}\frac{u_T{}^2}{T_m{}^2}}\,.$$

The squared relative uncertainty of the temperature in °C appears with a coefficient $c(T_m)^2$, where

$$c(T) = \frac{T}{273.15 + T}$$

is called the sensitivity coefficient of the temperature in this measurement. In the present example, it takes a value 0.08, and will be used below.

Uncertainty budget – initial version

Let us summarise the steps in the process as we have developed it so far.

- The output result of a measurement depends on various inputs, termed influence quantities. Some of these are measured, some are not. We write down the relationship between the inputs and output: this defines our measurement model. In our example, the model is
$$k_{TP} = \frac{101.325}{p}\frac{(273.15 + T)}{293.15}$$
- For each influence quantity, we consider the possible sources of uncertainty. We make Type B estimates for them all, and obtain Type A estimates where appropriate.
- The contribution of each influence quantity to the standard uncertainty of the measurement output result is obtained using sensitivity coefficients derived from the model equation.
- These standard uncertainty contributions are summed in quadrature.

This calculation should be presented in a table, sometimes referred to as an uncertainty budget, as follows. The table has one heading for each quantity appearing in the model: these are the influence quantities, which we name. For each one, we quote its value and, for each source of uncertainty, our estimate and sufficient detail about the estimate to derive a standard uncertainty, usually by application of a reducing factor *k*. Sometimes this means we have to specify the probability distribution that we ascribe to each influence quantity. We also give the sensitivity coefficients and, in the last column, the product of the standard uncertainty and the sensitivity coefficient. This product is the uncertainty component arising from each source in the standard uncertainty of the quantity being measured. The sum in quadrature of these uncertainty components appears in the last row. The whole calculation is conveniently carried out in a spreadsheet so that intermediate results are retained with full precision. In this way, the effect of rounding is postponed until the last step.

Note	Quantity, source of uncertainty	Value of quantity	Expanded uncertainty	Type of uncertainty	Confidence level	Coverage factor	Standard uncertainty	Sensitivity coefficient	Uncertainty component	Working
			U_i			k	u_i	c_i	$\|c_i u_i\|$	
	Pressure (kPa)	102.30								
1	calibration		0.1	B	95%	2	0.05%	1.00	0.05%	2.4×10^{-7}
2	repeatability		0.03	A	68%	1	0.03%	1.00	0.03%	8.6×10^{-8}
3	resolution		0.005	B	100%	1.73	0.003%	1.00	0.003%	8×10^{-10}
4	Temperature (°C)	23.4								
5	calibration		0.5	B	95%	2	1.07%	0.08	0.08%	7.1×10^{-7}
6	resolution		0.1	B	100%	1.73	0.25%	0.08	0.02%	3.8×10^{-8}
	Air density	1.0020								
7	combined						0.10%			1.1×10^{-6}

Table 1 Uncertainty budget – initial version

Notes

1. The barometer has a certificate in which the (additive) calibration is given as – 0.2 kPa ± 0.1 kPa, where the uncertainty is based on a coverage factor k = 2, stated to correspond approximately to a confidence level of 95%. Each pressure reading is affected in the same way and so, in the present context the calibration makes a contribution to the uncertainty of Type B. We use k as a reducing factor to obtain the standard uncertainty (0.05 kPa), and express this relative to the measured value (0.05%).
2. The mean pressure reading has an uncertainty which makes a type A contribution, as worked out in Example 2 above.
3. The resolution of the barometer, which reads to the nearest 0.01 kPa, is such that it makes a negligible contribution to the uncertainty, unlike the thermometer (note 6 below). In preparing an uncertainty budget, it is essential to note which sources of uncertainty have been considered. When, as in this case, the contribution is negligible, one may omit the contribution from the table.
4. In this example, the mean value of temperature readings has vanishing Type A uncertainty.
5. The thermometer's (additive) calibration, 0.6 °C ± 0.5 °C (based on a coverage factor k = 2, and stated to correspond approximately to a 95% confidence level), is handled similarly to the barometer calibration. We reduce it to a standard uncertainty, relative to the measured value in °C, and include the required sensitivity coefficient.
6. In this example, the effect of limited resolution in the temperature measurement is not negligible, and an uncertainty contribution of Type B arises. In this case, the coverage factor is $\sqrt{3}$.
7. Each uncertainty contribution is squared (the working is shown in the last column, normally omitted) and summed to produce the squared relative uncertainty of the measurement result (in the same column). The standard uncertainty (0.10%) of the result follows on taking the square root and rounding appropriately.

Quantities that influence ionisation measurements

Influence quantities are those that are not the subject of the measurement but yet affect the reading of the dosemeter (e.g. air pressure, ageing and zero drift of the electrometer, beam quality, dose rate, field size, etc.) In measuring ionisation, as many influence quantities as practicable should be kept under control and, for the rest, their effects should be measured and corrected for. Incomplete knowledge of these effects will contribute to the uncertainty of the measurement, and the uncertainty budget provides a systematic way to consider them all. In practice, one should set a reasonable limit for the smallest uncertainty to be included in the analysis (e.g. 0.1%). In preparing an uncertainty budget, a calibration laboratory will list these negligible sources in order to document the fact that they were not merely forgotten. Quantities to consider include the following:

- **Air density (pressure and temperature)**

The barometer should be calibrated and located in the same room, or at least on the same floor as the ionisation chamber. The temperature of the air inside the ionisation chamber cavity is not so easy to measure, but at equilibrium it should be close to that of the surrounding phantom (if any). Much of the uncertainty from air density tends to cancel in carrying out a cross calibration, though not in a measurement of machine output.

- **Humidity**

Dry air is slightly more dense, the energy required to produce an ion pair is slightly larger in dry air, and the electron mass-stopping power is slightly affected by humidity. However these effects tend to cancel and, for a graphite-walled ion chamber, the overall change in response is less than 0.1% provided the relative humidity lies between 20% and 70%, for temperatures between 15 ºC and 25 ºC.

- **Stabilisation**

Electronic instruments take time to warm up, especially mains-powered ones. In addition to the effects of temperature, the charge collection efficiency of an ion chamber usually drifts slightly during the first few minutes after the polarising potential is applied. For NE2571 chambers, we have found that this settling is usually complete once a pre-calibration dose of 4 Gy has been given. Best practice would be to record readings during this initial dose, to produce evidence that the chamber has settled before measurements begin.
Longer term stability of the instrument can be monitored using a ^{90}Sr check source.

- **Leakage**

The polarising voltage tends to generate a small current, even in the absence of radiation, because no electrical insulator is perfect. Leakage can also be radiation induced, and be affected by humidity. In therapy-level measurements, the leakage current should normally be less than 0.1% of the measured value, except possibly when using very small volume ion chambers. Dirty connectors can cause excessive leakage. Use the dust caps!

- **Ion recombination**

This is generally small except for pulsed beams (see the electron dosimetry practical session). Sometimes the calibration is valid for chamber readings which have *not* been corrected to zero ion recombination (e.g. air kerma, which is generally measured in continuous beams, where the recombination is small and independent of dose rate). Such a calibration is sometimes said to "include recombination" but this phrase can be a source of confusion: it is better to specify the readings, corrected or not, for which a calibration is valid.

- **Polarity effect**

The response of an ion chamber may change significantly when the sign of the polarising potential is changed, especially in electron beams (including beta sources like a ^{90}Sr check source). As with ion recombination, you need to be clear how the calibration is defined. The NPL calibration for photon measurements is valid for readings with negative polarity (and you need to be clear what this means), while the electron beam calibration is valid for readings averaged over negative and positive polarity. The chamber polarity is the sign of the charge collected and measured, though only a few types of measuring assembly display a minus sign when it should be there.

- **Radiation beam geometry**

Detector response usually depends on the angular and energy distribution of the radiation, which both vary with collimator setting. For this reason, ion chambers should be set up and aligned carefully with the beam. Conventional reference conditions (10 cm square field) avoid the increased uncertainty associated with dosimetry in small fields, where there may be steep dose gradients.

- **Radiation beam quality**

Beam quality refers to the penetrating power of the radiation, which in radiotherapy affects the dose distribution within the patient. The beam quality parameter (whether HVL, TPR, or R_{50}) is also used to label the beam in which an ion chamber is calibrated. There remains some small uncertainty when transferring an ion chamber calibration from one beam to another, even if the quality parameters of the beams are matched.

- **Output variations**

The use of a monitor chamber should reduce the effect of changes in machine output, although note that the monitor is usually located away from the point of interest (e.g. at depth in a phantom). In the case of a ^{60}Co unit, one should consider transit time effects.

Higher levels of confidence

So far we have obtained a standard uncertainty *u* for our air density correction, and know that this corresponds to a confidence probability of about 68%, at least if our measurement has a gaussian distribution. But what if we want to quote an uncertainty with a greater level of confidence, i.e. an expanded uncertainty *U*: how are we to choose a value for *k*?

If we were sure that our measured quantity has a gaussian distribution, and also sure about our value for the standard uncertainty, then we could obtain a 95% confidence interval by taking $k = 2$.

On the other hand, if we are not so sure about the value of *u*, then it is fairly clear that taking $k = 2$ would produce an interval about which we must have less than 95% confidence. This means we ought to choose *k* to be somewhat larger than 2 to compensate for this doubt.

The question emerging here is: *What is the uncertainty of the uncertainty?*

In order to answer this question about the combined standard uncertainty in the last row of our table, it is evident that first we need to know how sure we are about each of the component uncertainties in the lines above.

Degrees of freedom

Rest assured, this is not the beginning of an infinite regress: our uncertainty statement will be complete when it includes an indication of how sure we are of the uncertainty value itself. The analysis above is extended to cover the "effective number of degrees of freedom" ν_{eff} for each of the component sources of uncertainty, and also for the combined uncertainty of the result. We postpone for a moment going into detail about the method for combining degrees of freedom and return to the pressure measurement which was based on a series of $N = 10$ readings. We evaluated the standard deviation of these readings and used this as an estimate (4) of the standard deviation of the distribution from which the readings come. The larger *N* is, the more reliable this estimate will be. One can think of the "uncertainty on the uncertainty" (5), as being proportional to $\frac{1}{\sqrt{\nu}}$.

It turns out that our estimate (4) has its own probability distribution, called a Student's t-distribution. The width of the distribution containing p % of the values is $\pm t_p$. The distribution has a parameter, called the number of degrees of freedom, defined to be $\nu = N - 1$, the factor appearing in the denominator in equation (4). The larger ν is, the closer the t-distribution approaches a gaussian. For values of ν that are not so large, more of the probability spreads out into the tails of the distribution. The coverage factor *k*, for an uncertainty component with confidence probability *p* and ν_{eff} effective degrees of freedom is none other than the value t_p for the t-distribution with that many degrees of freedom. Some values of the t-distribution are given here:

v	68%	95%	99%
1	1.8	12.7	63.7
2	1.3	4.3	9.9
3	**1.2**	**3.2**	**5.8**
4	1.1	2.8	4.6
5	1.1	2.6	4.0
6	1.1	2.4	3.7
8	1.1	2.3	3.4
10	**1.0**	**2.2**	**3.2**
15	1.0	2.1	2.9
20	1.0	2.1	2.8
30	**1.0**	**2.0**	**2.7**
50	1.0	2.0	2.7
100	**1.0**	**2.0**	**2.6**

Table 2 Selected Student's t values

It is less obvious what to do for Type B uncertainties but, following Bentley's monograph, we proceed pragmatically. A large number of degrees of freedom implies that we are quite sure about our estimate of the standard uncertainty, while a small number of degrees of freedom means we are much less sure. Once the degrees of freedom of all uncertainty contributions have been combined it turns out that, in nearly all cases, the effective number of degrees of freedom of the result is insensitive to the values of ν_{eff} for most components. This means that we can get away with the following idea. We distinguish between uncertainty estimates that we judge to be "excellent", "good", "rough" or "poor", and assign them effective degrees of freedom equal to 100, 30, 10 and 3 respectively. We make no finer distinction that this.

Equipped with such a scheme for assigning effective degrees of freedom to each uncertainty component, we return to consider the question how these degrees of freedom may be combined.

Combining effective degrees of freedom

The uncertainty contributed by each influence quantity is $c_i u_i$, and these are summed in quadrature to give the combined uncertainty, u, according to

$$u^2 = \sum_i (c_i u_i)^2 \ . \qquad (6)$$

Our example takes this form with the index *i* corresponding to the two quantities pressure *p* and temperature *T*. At risk of confusion, but just for a moment, we treat this equation (6) as a (measurement) model in its own right, and ask how the *uncertainty* of the result (i.e. of the left-hand-side) is determined by the *uncertainties* of the terms in the sum on the right. Each term, we have suggested, has an uncertainty proportional to $\sqrt{\frac{1}{\nu_i}}$, where ν_i is the effective number of degrees of freedom for that source of uncertainty. In fact our estimate is that the uncertainty in $(c_i u_i)^2$ is equal to $(c_i u_i)^2 / \sqrt{\nu_i}$.

Since uncertainties add in quadrature, this implies that the *squared* uncertainty of the RHS in equation (6) is $\sum_i (c_i u_i)^4 / \nu_i$. This sum we equate to the squared uncertainty of the LHS, which we write in the same form, u^4 / ν_{eff} :

$$u^4 / \nu_{eff} = \sum_i (c_i u_i)^4 / \nu_i ,$$

so that the effective number of degrees of freedom of the combined uncertainty is given by

$$\nu_{eff} = u^4 / \left(\sum_i (c_i u_i)^4 / \nu_i \right),$$

a formula due to Welch and Satterthwaite.

Uncertainty budget (final version)

The initial version of our uncertainty budget can now be extended to include a column in which we enter the effective number of degrees of freedom for each source of uncertainty. The calculation by which we arrive at the effective number of degrees of freedom for the measurement result, ν_{eff} , may conveniently be carried out in further columns to the right, as in Table 3. Having obtained ν_{eff} , the expanded uncertainty for a coverage probability *p* may be obtained by identifying the coverage factor *k* with t_p, taken from the corresponding t-distribution. As before, the right hand part of the table would not normally be shown and is given here only by way of clarification.

Rounding

In the final expression of measurement uncertainty, the value and its uncertainty should be rounded to the same precision, as in

> The air density correction was measured to be $k_{Tp} = 1.0020 \pm 0.0021$, with a confidence probability of 95%. The coverage factor for the interval is $k = 2.00$.

In many cases, one significant digit in the uncertainty is enough. Only where the leading digit is a 1 or 2 might there be a strong case for greater precision in the uncertainty. Rounding should only be applied to the final result and its uncertainty, not at intermediate steps in the analysis.

Note	Quantity, source of uncertainty	Expanded uncertainty	Type of uncertainty	Confidence level	Coverage factor	Standard uncertainty	Uncertainty component	Effective degrees of freedom				
		U_i			k	u_i	$\lvert c_i u_i \rvert$	ν_{eff}	$\lvert c_i u_i \rvert^2$	$1/\nu_{eff}$	$\lvert c_i u_i \rvert^4$	$\lvert c_i u_i \rvert^4 / \nu_{eff}$
	Pressure (kPa)											
1	calibration	0.1	B	95%	2	0.05%	0.05%	30	$2.4\text{x}10^{-7}$	$3.3\ \text{x}10^{-2}$	$5.7\ \text{x}10^{-14}$	$1.9\ \text{x}10^{-15}$
2	repeatability	0.03	A	68%	1	0.03%	0.03%	9	$8.6\text{x}10^{-8}$	$1.1\ \text{x}10^{-1}$	$7.4\ \text{x}10^{-15}$	$8.2\ \text{x}10^{-16}$
3	resolution	0.005	B	100%	1.73	0.003%	0.003%	100	$8\text{x}10^{-10}$	$1.0\ \text{x}10^{-2}$	$6.3\ \text{x}10^{-19}$	$6.3\ \text{x}10^{-21}$
	Temperature (°C)											
5	calibration	0.5	B	95%	2	1.07%	0.08%	30	$7.1\text{x}10^{-7}$	$3.3\ \text{x}10^{-2}$	$5.1\ \text{x}10^{-13}$	$1.7\ \text{x}10^{-14}$
6	resolution	0.1	B	100%	1.73	0.25%	0.02%	100	$3.8\text{x}10^{-8}$	$1.0\ \text{x}10^{-2}$		
	Air density											
7	combined	0.0021	combined	95%	2	0.10%		59	$1.07\text{x}10^{-6}$	$1.8\ \text{x}10^{-2}$	$1.1\ \text{x}10^{-12}$	$2.0\ \text{x}10^{-14}$

Table 3 Uncertainty budget – final version

Notes

Two columns have been omitted (Value of quantity, sensitivity coefficient) in order to show the last four columns in detail

All of the remarks made in the notes to Table 1 apply to the final version of the uncertainty budget in Table 3. In addition, we note that:

1. The number of degrees of freedom might be stated explicitly in the calibration certificate. If it is not one can, in principle, take the confidence level (95%) and coverage factor ($k = 2$) at face value and work backwards, using tables of Student's t-distribution and infer a value of 60. Here we adopt the same approach as for the other type B contributions and choose the value 30, which represents a "good" estimate of uncertainty.
2. The effective number of degrees of freedom for the uncertainty on the mean of *N* readings, a type A estimate, is just $N - 1$, here equal to 9.
3. The barometer resolution is not in doubt, and so the uncertainty estimate is "excellent". Any increase of ν_{eff} for this contribution beyond our conventional value 100 would have a completely negligible effect on the final uncertainty and its number of degrees of freedom.
5. The same remarks apply as for note (1).
6. Likewise, note (3), except that in this case the contribution is merely small, rather than completely negligible.
7. The formula for the effective number of degrees of freedom will in general yield a non-integer value. It must be rounded to an integer in order to use the t-distribution, either tabulated as in the text, or using a formula in a spreadsheet program. This is the only point in the calculation where it is necessary to round an intermediate result.

Postscript – uncertainty budgets in use

A useful analogy exists between an uncertainty budget and a financial budget: it is an allowance to be used, but not necessarily to be used up, and it should definitely not be exceeded. It is not essential to go through a fresh uncertainty analysis every time a routine measurement is performed. Rather, uncertainties should be analysed in the way described here when the measurement procedure is drawn up. As experience is gained in following the procedure and as measurement data accumulate, it becomes possible, and even preferable, to replace some of the component uncertainty estimates (ones based on actual readings taken during a particular measurement) by typical, if conservative, values based on experience with many instruments of the type in use. This experience should be incorporated into acceptance criteria (tolerances) for the measurements which, if they are not met, will indicate that a problem exists. These criteria may be refined as further data are acquired.

Note that where a calibration laboratory achieves accreditation, this will be for the provision of a service to a specified uncertainty. It would be a non-compliance for an accredited laboratory to issue a calibration certificate with an uncertainty which is better than that specified in the accreditation. In the terms of the analogy above one should in such a case, rather than issue a certificate with an uncertainty which is “too good”, report a conventional value for the uncertainty (for which the service has been accredited) knowing that on this occasion at least, the budget has not been exhausted.

References

International Organization for Standardization, *Guide to the Expression of Uncertainty in Measurement*. ISO, Geneva (1995).

A user-friendly version of ISO guide is presented in the monograph

Robin E Bentley, *Uncertainty in Measurement: The ISO Guide*, National Measurement Laboratory, CSIRO, Australia.

A concise summary of the GUM approach is contained in Appendix A of:

International Atomic Energy Agency, TRS 398, *Absorbed Dose Determination in External Beam Radiotherapy*, IAEA (2000), Vienna.

Attix, F H (1986) *Introduction to Radiological Physics and Radiation Dosimetry*, John Wiley and Sons, Inc.

Klevenhagen, S C (1985) *Physics of Electron Beam Therapy*, The Institute of Physics.

The most up-to-date survey of the calorimetry are the following proceedings:

Proceedings of NPL Workshop on Recent Advances in Calorimetric Absorbed Dose Standards Eds Williams, A J and Rosser, K E (2000), NPL Report CIRM 42.

Proceedings of a Workshop on Recent Advances in Absorbed Dose Standards ARPANSA, Melbourne, August 2003, *Eds Huntley, R B and Webb, D V* available online at http://www.arpansa.gov.au/absdos/proc.htm.

ICRU report 64 (2001) Dosimetry of high-energy photon beams based on standards of absorbed dose to water, *International Commision on Radiation Units and Measurements report 64*, (Nuclear Technology Publishing, Ashford)

Many countries including the UK maintain national protocols for dosimetry, but the recent IAEA code is currently the most up-to-date and review:

International Atomic Energy Agency, TRS 398, *Absorbed Dose Determination in External Beam Radiotherapy*, IAEA (2000), Vienna.

Maintenance and general care of secondary standard and field instruments

This is without doubt the most important lecture that you will be given during this course. That rather rash statement is based on the fact that you may be the best physicist in the world but if the equipment you are using does not work correctly then any measurements that you make will be worthless.

In these sessions we will cover the following areas:

Session A

General care of equipment

This will cover issues concerning how instruments should be stored and maintained, cleaning of instruments and general physical (external) checks. The session will introduce the different instrument types that will be used in the practical sessions, covering any specific points associated with individual items, giving an opportunity for students to familiarise themselves with the operation of any items new to them.

Checking equipment is operating properly for in-beam measurements

Here we will cover checks for both radiation and non-radiation induced leaks, checks for contamination and degradation of component parts such as radiographing of chambers to reveal possible internal damage and the identification of problems through long-term observation of an instrument's performance.

Session B*

**This will be carried out as part of the kV X-ray practical session*

Setting up and carrying out a check source measurement

Here you will have the opportunity to carry out examinations and check source measurements of all the instruments available. This will allow you to check that the instrument is in a fit condition for use and to demonstrate the correct set up and operation of the instrument. We will also discuss factors affecting the time required for instruments to settle (thermal, electrical etc); calibration and specification requirements of associated equipment such as barometers and thermometers; familiarisation with calibration certificates associated with the instruments to be used; discussion of levels of uncertainties and agreement between measurement readings.

Session A

1 General care of equipment

All the instruments used at NPL whether secondary or tertiary standards are expensive to buy and by the time they have been calibrated a lot of very precious time has been invested in them. Despite this when we visit hospitals and laboratories it is not uncommon to see an instrument stored under a desk where it gets kicked or knocked every time someone sits down, or tucked in the corner acting as a door stop. Instruments should have a designated storeroom

or cupboard, preferably lockable, where they can be kept (try not to use the cupboard that has the central heating pipes running through it)! When you have found a cosy and safe place for your instrument remember to look after it. As time goes by, much like us, bits age and drop off! So to keep your equipment "healthy", here is a simple checklist to follow. This is not intended as a definitive list and will depend on the instrument type.

1.1 Instrument Check List

1.1.1 Chamber

Visual Inspection:

a) Make sure that the chamber is properly stored.
b) Regularly carry out a physical check of the chamber construction (e.g. check that the cap, outer casings and retaining nuts are not loose, that the pins in the outer stem of a 2561 have not fallen out etc).
c) Check for signs of any contamination (e.g. talcum powder, hand cream).
d) Keep cables / connectors / dust caps clean and free from damage and replace any missing components.
e) Look after the chamber case. Keep it clean and secure (some cases become self-opening!).
f) Get to know your chamber. Is there anything that doesn't look right?

Operational:

g) Always give the chamber a pre-irradiation dose before each use.
h) Check for signs of any leaks (natural, radiation induced).
i) Carry out regular check source measurements.
j) Keep a history of the chamber response to allow you to check its' long term stability.
k) Carry out regular radiographs of your chamber. These can reveal problems even in brand new chambers.

1.1.2 Measuring Assembly

Visual Inspection:

a) Make sure that the measuring assembly is properly stored.
b) Check the desiccator regularly and dry it out if suspect.
c) Keep cables / connectors / dust caps clean and free from damage and replace any missing components.
d) For battery operated instruments, check that the batteries are in good condition and do not need replacing (before leaking occurs inside the instrument!)
e) Ensure that the cases and their lids and handles are secure (and there is nothing rattling around inside the case).

Operational:

f) Check that the charge and/or current calibration are correct.
g) Always carry out a self-check on the instrument if available (e.g. Dosemaster).
h) Always ensure that the HT supply to the chamber is the correct value.
i) Check regularly for any leakages and drifts.

1.1.3 Check source

a) Make sure that the source is properly stored.
b) Regularly carry out a physical examination of the source (e.g. has it been dropped).
c) Check that all parts are present (such as tamper-proof disc on base of source / source feet / source plugs etc) and replace any missing components.
d) Keep the storage and transport case in good condition and make sure it conforms to current transport regulations.
e) Regularly carry out radioactive leak tests.

All the instruments covered on this course have the same basic function of measuring the ionisation produced in the ion chamber volume resulting from the incident radiation beam. This can be determined by measuring the collected charge as with the secondary standard NE 2560 or by measuring the current as with the NE 2670. However there may be subtle variations between types, even between instruments of the same type, and user interfaces between manufacturers can be very different. It is therefore advisable to familiarise yourself with the fundamental mode of operation of your own specific equipment.

1.2 Instrument types

Instruments that will be used on the course will include the following:

1.2.1 Ionisation chamber types

- NE 2561/2611
- NE 2571
- NE 2502
- Wellhofer “Farmer” type both standard and waterproof
- Very low energy thin window chambers;
- NACP, ROOS and Markus parallel plate electron chambers

1.2.2 Measuring Assembly types

- NE 2560
- NE 2570
- NE 2670
- NE Dosemaster
- PTW Unidos
- Wellhofer dose 1

1.2.3 Radioactive Check Source types

- NE 2562
- NE 2606
- NE 2503
- PTW 8921

2 Checking equipment is operating properly for in-beam measurements

2.1 Natural Leak

A natural leak can occur in the instrument in the absence of a radiation field. To test for a natural leak after the instrument has been set up, unearth the electrometer and watch the reading for a period of time similar to that for which a normal reading would be taken. Record the reading at the start and watch what happens to it during the measurement, an “earthing kick” may sometimes occur immediately after pressing the start button. Record the final reading and repeat a few times to ensure consistency. If the drift is not considered negligible then the actual readings should be corrected. Large leaks or drifts may typically arise from:

- dirty connectors
- “wet” desiccators
- not giving instruments long enough to settle
- not giving a pre-irradiation dose to the chamber

2.2 Radiation induced leak

A radiation-induced leak is associated solely with the chamber and is identifiable only after the chamber has been exposed to a radiation field. If a radiation induced leak is present, there is usually a continued collection of charge even after the beam has been switched off, at a similar rate to that of the reading, which quickly levels off. Radiation induced leaks vary in their magnitude but provided they are small may be ignored. However, a chamber that exhibits a large leak will usually require repair by the manufacturer.

2.3 Contaminated and corroded chambers

The importance of recording the historical performance of a chamber is born out by the effects that may occur through contamination or corrosion and degradation. At the lower energy range this may be particularly noticeable. Each time a chamber is calibrated here at NPL we compare its performance against its response in previous calibrations.

NB: please let us know if a chamber has been repaired since its last calibration, it saves our time and your money!

A small shift in the calibration curve up or down is not unexpected, however a large shift or rotation of successive calibration curves may indicate a problem.

The graph in Figure 1 shows a customers secondary standard NE 2561 chamber that had been calibrated successfully with good agreement on two occasions (Autumn 1976, 1979). On its third visit to NPL a significant change in its response at lower energies was observed with a difference of 1.7% at the 2mm Al HVL, with no significant difference at higher energies (Before repair, 1982). On removal of the graphite cap, traces of a white deposit were found near to the vent hole and inside the cavity. When cleaned and the cap replaced it can be seen that the response of the chamber returned close to that previously observed (After repair, 1982). The contaminant was suspected to be talcum powder, probably from a waterproof latex sheath of a type that is now seldom used.

Again in Figure 2 we see an NE 2561 chamber that has shown good agreement between its first two calibrations with a difference of the order of 20% on its third visit. Interestingly the Strontium 90 check source measurements revealed no problem, showing good agreement between all three visits.

Q. Why was no difference observed in the Strontium 90 check source measurements for this chamber?

A radiograph of the chamber, and its subsequent dismantling, revealed that the hollow aluminium central collecting electrode, which has a wall thickness of 0.2mm had suffered severe corrosion resulting in a hole. Once the electrode was replaced, the chamber was recalibrated exhibiting a similar response to previously. After discussion with the owner it was concluded that the corrosion was due to the very high humidity in the store where the chamber was kept.

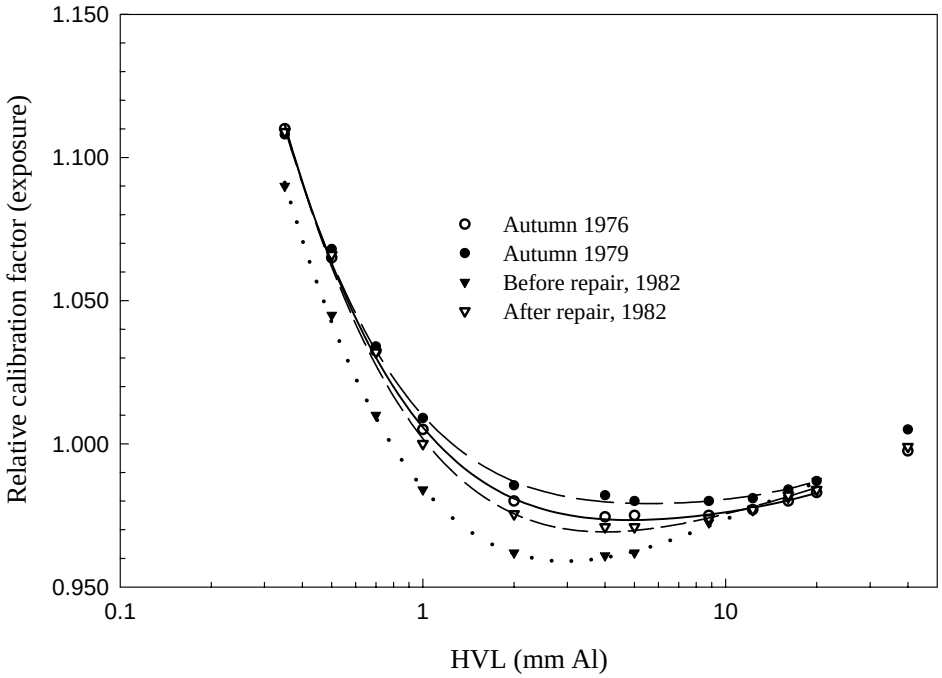

Figure 1 shows the effect of contamination, most likely talcum powder, on a Secondary Standard NE 2561 chamber.

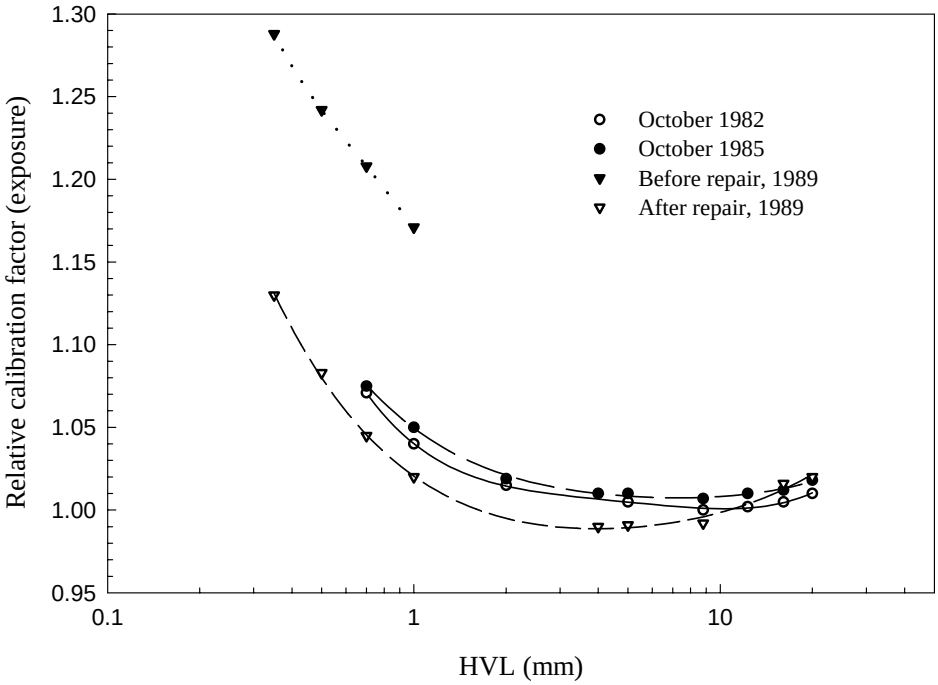

Figure 2 shows the effect of electrode corrosion due to poor storage conditions, on a Secondary Standard NE 2561 Chamber.

2.4 Radiographs

Radiographing a chamber is an extremely useful way to investigate possible problems without having to resort to dismantling the chamber, which would inevitably result in the invalidation of the calibration. Here are a number of radiographs that have been taken of chambers that have exhibited strange behaviour.

When commissioning a new chamber it is recommended that radiographs be taken to check that the design is consistent with the manufacturer's drawings and specification.

Q. Figures 3 and 4 both show brand new chambers that exhibited poorer than expected performance. Can you see why?

The chambers in Figures 5-7 are all NE 2561 secondary standard chambers, one is a routine radiograph and the chamber had no problems. The other two

both gave inconsistent readings in check source measurements and in high and low energy beams.

Q: The "good" chamber is shown in Figure 5, can you identify the problems with the other two chambers?

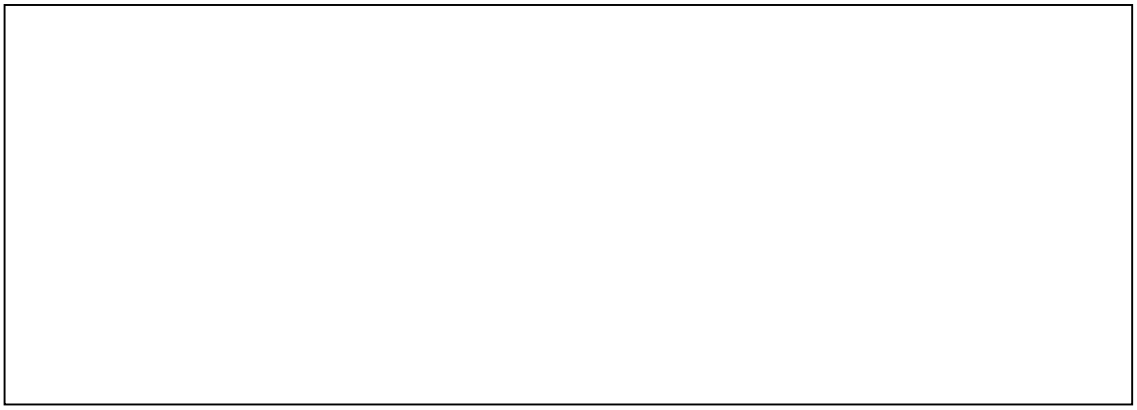

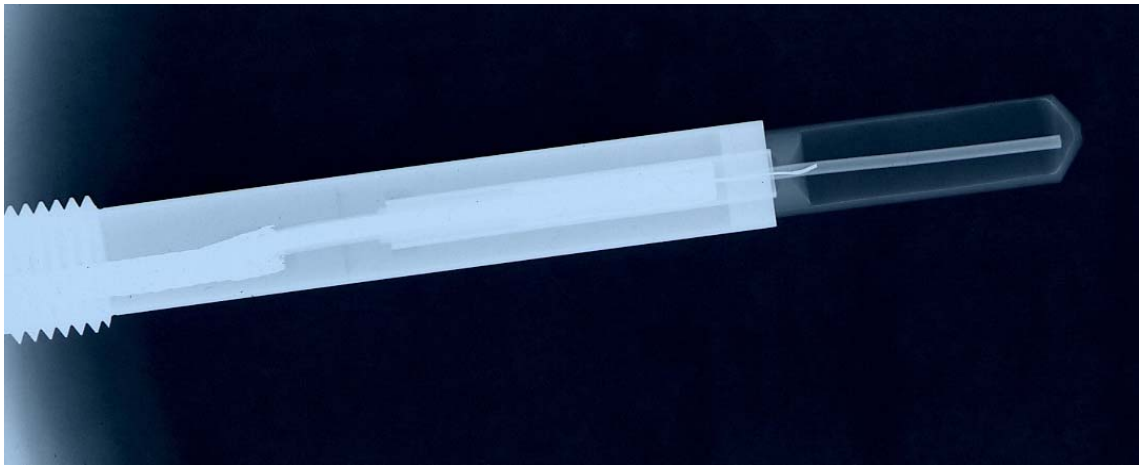

Figure 3 shows a “Farmer” type chamber with two obvious problems.

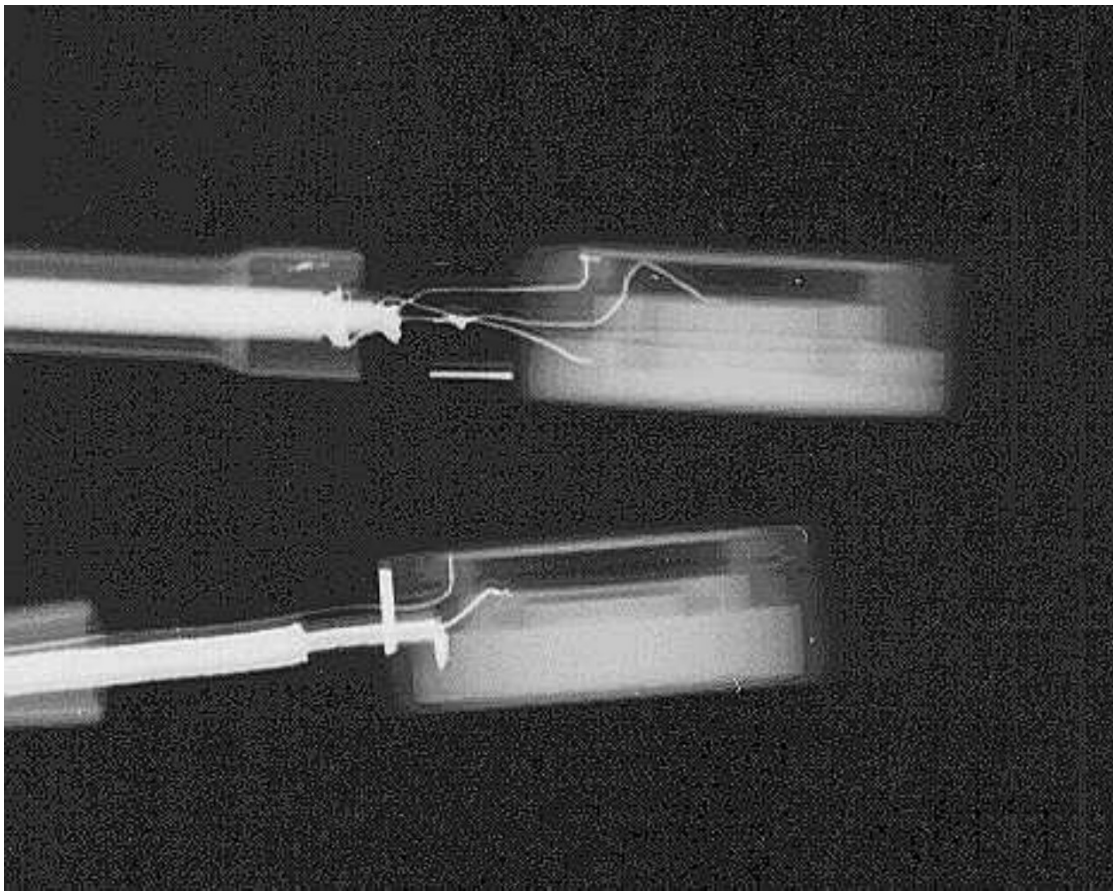

Figure 4 shows side-on radiographs of two NACP type chambers from different manufacturers. The lower one is correct the upper chamber is not and has a fault that would seriously affect its performance.

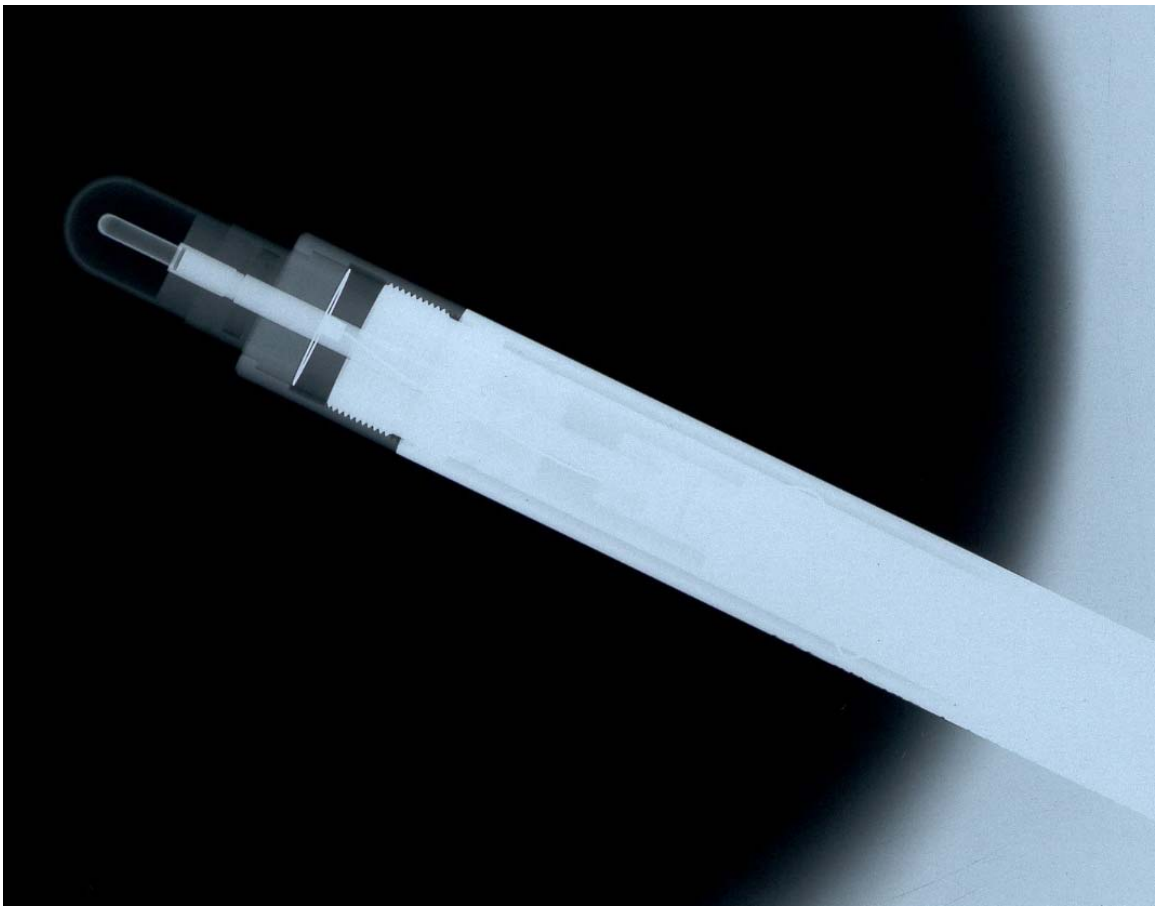

Figure 5 shows an NE 2561 chamber that is operating correctly.

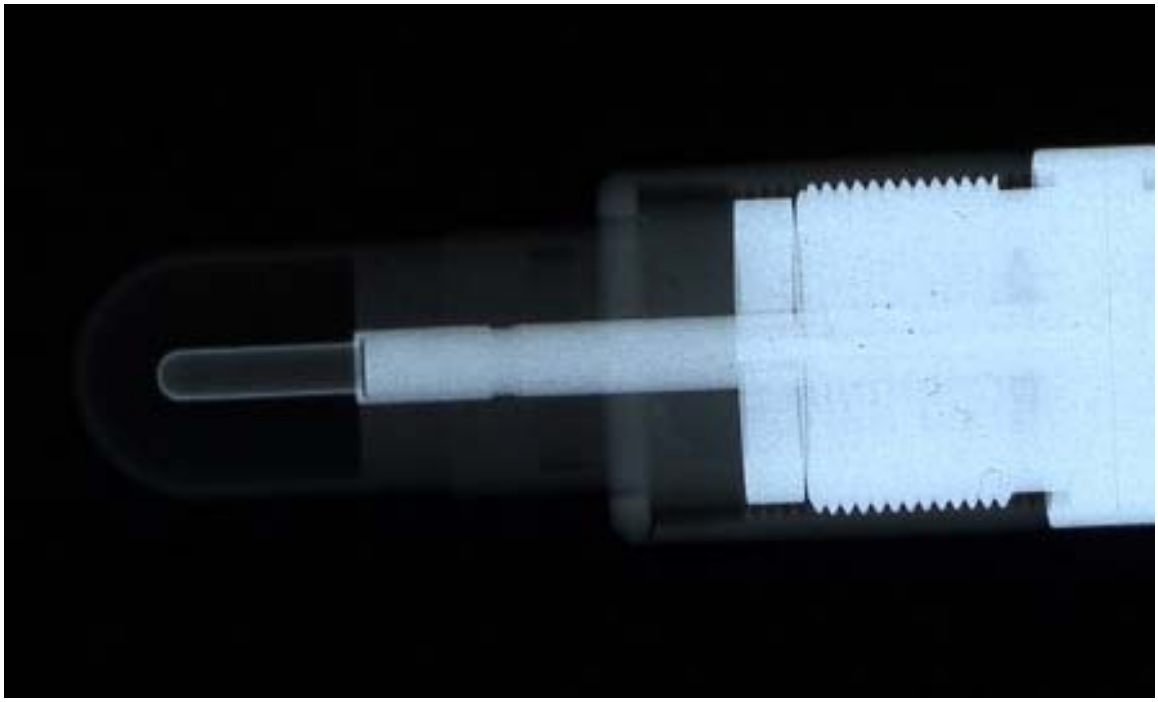

Figure 6 shows an NE 2561 chamber with…?

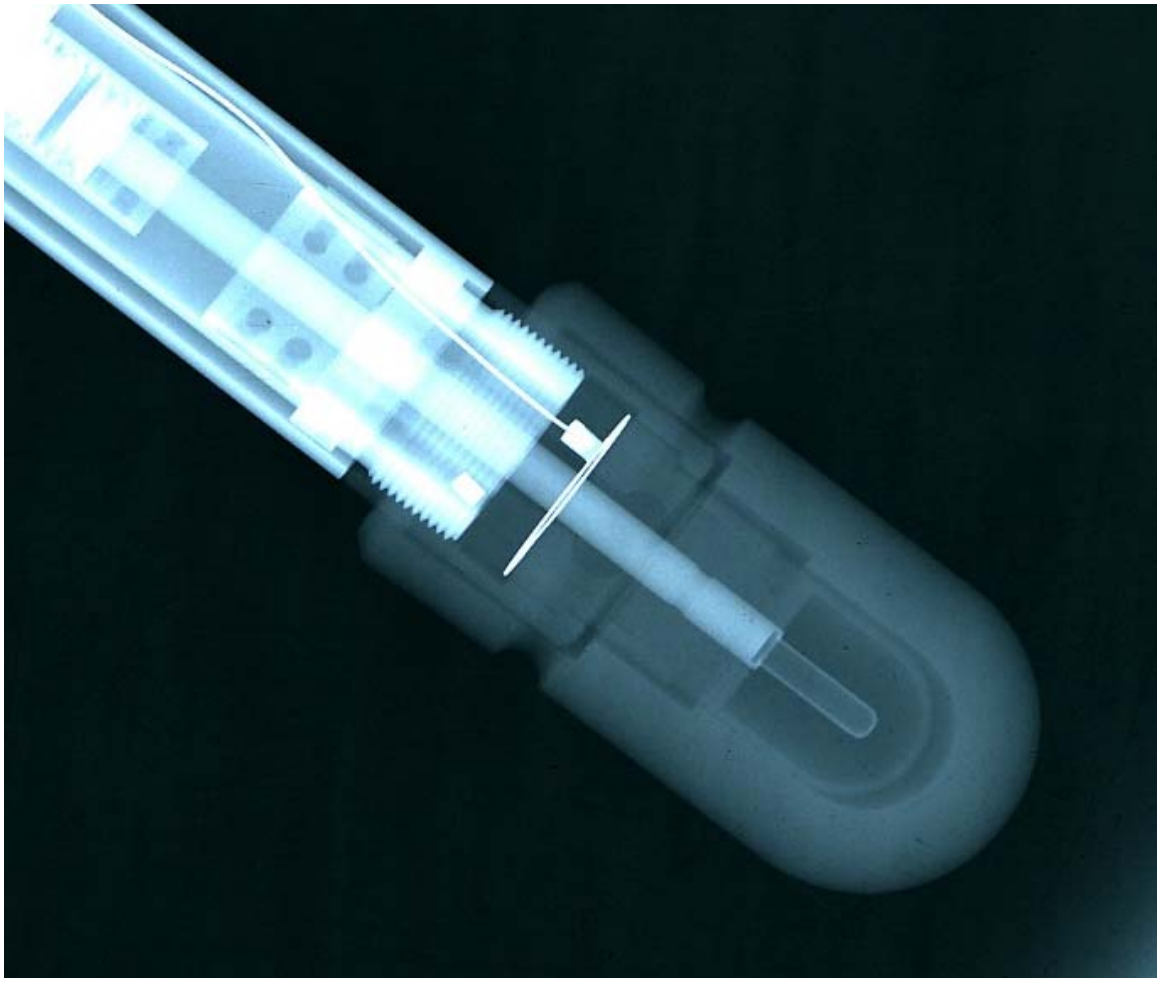

Figure 7 shows an NE 2561 chamber with…?